DISSERTATION

On

"Study of Seismic Response of Rectangular Water Tank"

Submitted by

Rama Pandey
M.Tech. (Structural Engineering)
2K13/STE/15

Under the guidance of

Mr. Alok Verma
Associate Professor
(Department of Civil Engineering)
Delhi Technological University

Department of Civil Engineering
Delhi Technological University (D.T.U.), Delhi-110042

June 2015

CERTIFICATE

This is to certify that the report entitled "STUDY OF SEISMIC RESPONSE OF RECTANGULAR WATER TANK" is being submitted by me, which is a bonafide record of my own work under the guidance and supervision of my project guide Mr. Alok Verma, in the partial fulfilment of requirement for the award of the degree of Master of Technology (M.Tech.) in Structural Engineering, Department of Civil Engineering, Delhi Technological University (D.T.U.), Delhi.

The matter embodied in the project has not been submitted for the award of any other degree.

Rama Pandey

2K13/STE/15

This is to certify that the above statement made by the candidate is true to the best of my knowledge and belief.

Alok Verma

Associate Professor

Department of Civil Engineering

D.T.U., Delhi

ACKNOWLEDGEMENT

I would like to express my sincere gratitude to my project guide Mr. Alok Verma (Associate Professor, Delhi Technological University) for giving me the opportunity to work on this topic. It would never be possible for me to complete this project without his precious guidance and his relentless support and encouragement.

I would also like to present my sincere regards to my Head of Civil Engineering Department Dr. Nirendra Dev , for his support and encouragement throughout the programme.

I am also thankful to all the faculty members and my classmates for the support and motivation during this work.

Last but not least, I specially thank all the people who are active in this field. Reference material (pictures, tables and forms) from various national and internal reports and journals are included in this report as per requirement and all these are quoted under the reference section at the last of this report.

RAMA PANDEY

ROLL NO-2K13/STE/15

M TECH

STRUCTURAL ENGINEERING

ABSTRACT

Water tanks are very important structures and consist of various types. Such tanks become vital structures after a seismic activity for providing potable water supply and in controlling earthquake generated fires. Elevated tanks get heavily damaged or even collapse during earthquakes. Tanks are also utilized to store various types of products, for example petroleum supplies in cities and industrial areas. Damages to these structures during high seismic activities may lead to many hazardous events. Therefore storage tanks should stay functional during and after earthquakes. Seismic behavior of storage tanks including movement of stored liquid has attracted attention of many researchers. Their dynamic behavior has been found to be different in comparison to other structures.

The seismic behavior of storage tank is affected by various factors like soil-structure interaction, structural parameters, earthquake characteristics, the supporting system etc. Experiences show that inadequately designed or detailed liquid storage tanks, which are common structures in various facilities, suffered extensive damage during past earthquakes. Therefore, the satisfactory seismic response study of such structures is very important. The purpose of this project is to study and computationally examine the effects of earthquake frequencies on the seismic behavior of rectangular storage tanks. Phenomenon of sloshing of liquid in rectangular water tanks has been studied with and without baffles. Wooden baffles of different heights were used to affect sloshing with variation of initial liquid fill level relative to the baffle height.

The tank is excited with frequencies near to natural frequencies of the liquid in the tank at different modes. It can be observed that if the tank is subjected to seismic excitations at resonant excitation frequencies, liquid sloshing becomes extreme and wall forces are intensified. It is observed that baffles may affect sloshing of stored liquid inside tanks to a great extent. The maximum impact pressure for the tank with baffle is seen to be significantly reduced in comparison to a tank without any baffle.

LIST OF TABLES

Table 5.1: Equipments used in conducting experiment on water tank 31

Table 5.2: Variation of acceleration with time at 50% fill at f_n= 2.8Hz 46

Table 5.3: Variation of acceleration with time at 80% fill at f_n= 2.8Hz 47

Table 5.4: Variation of acceleration with time at 50% fill at f_n= 4.4Hz 48

Table 5.5: Variation of acceleration with time at 80% fill at f_n= 4.4Hz 49

Table 5.6: Variation of acceleration with time at 50% fill with 0.3m baffle at f_n= 2.8Hz 50

Table 5.7: Variation of acceleration with time at 80% fill with 0.3m baffle at f_n= 2.8Hz 51

Table 5.8: Variation of acceleration with time at 50% fill with 0.3m baffle at f_n= 4.4Hz 52

Table 5.9: Variation of acceleration with time at 80% fill with 0.3m baffle at f_n= 4.4Hz 53

Table 5.10: Variation of acceleration with time at 50% fill with 0.4m baffle at f_n= 2.8Hz 54

Table 5.11: Variation of acceleration with time at 80% fill with 0.4m baffle at f_n= 2.8Hz 55

Table 5.12: Variation of acceleration with time at 50% fill with 0.4m baffle at f_n= 4.4Hz 56

Table 5.13: Variation of acceleration with time at 80% fill with 0.4m baffle at f_n= 4.4Hz 57

Table 6.1: Natural frequencies of liquid contained in rectangular tank 58

LIST OF FIGURES

Figure 1.1: Linear wave motion 3

Figure 1.2: Fluid Structure Interaction 4

Figure 2.1: Collapsed elevated tank in Bhuj(India) 7

Figure 2.2: Elephant foot buckling of broad tank 8

Figure 2.3: Diamond buckling in slender tank 8

Figure 2.4: Damaged seals in tanks from sloshing of liquids 9

Figure 2.5: Oil tank sloshing spill over tank 9

Figure 2.6: Typical collapsed small steel water tank 9

Figure 2.7: Qualitative description of hydrodynamic pressure distribution 12

Figure 2.8: Housner's mechanical spring model for tanks 14

Figure 2.9: Anti-symmetric modes for rectangular tanks 14

Figure 3.1: Water tank model 17

Figure 3.2: Geometry of baffles used 19

Figure 3.3: Geometry of the tank with baffle 19

Figure 4.1: Liquid sloshing in membrane without baffle 23

Figure 4.2: Liquid sloshing in membrane with baffle 23

Figure 4.3: Geometry of water stored in rectangular tank 26

Figure 4.4: The first few modes of oscillations of the liquid surface 26

Figure 4.5: Equivalent mechanical system of simple oscillators 28

Figure 4.6: Equivalent mechanical system considering the first mode of oscillation 29

Figure 5.1: Experimental setup 31

Figure 5.2: Surface profile at first mode (f_n = 1.6Hz) 34

Figure 5.3: Surface profile at second mode (f_n = 2.8Hz) 35

Figure 5.4: Surface profile at third mode (f_n = 3.7Hz) 36

Figure 5.5: Surface profile at fourth mode (f_n = 4.4Hz) 37

Figure 5.6: Surface profile at 50% fill at frequency 2.8Hz with baffle height 0.3m 38

Figure 5.7: Surface profile at 50% fill at frequency 4.4Hz with baffle height 0.3m 39

Figure 5.8: Surface profile at 80% fill at frequency 2.8Hz with baffle height 0.3m 40

Figure 5.9: Surface profile at 80% fill at frequency 2.8Hz with baffle height 0.4m 41
Figure 5.10: Surface profile at 80% fill at frequency 4.4Hz with baffle height 0.4m 42
Figure 5.11: Surface profile at 50% fill at frequency 2.8Hz with baffle height 0.4m 43
Figure 5.12: Surface profile at 50% fill at frequency 4.4Hz with baffle height 0.4m 44
Figure 6.1: Accelerations at 50% fill at frequency 2.8Hz 58
Figure 6.2: Trend line for local maxima of accelerations at 50% fill at frequency 2.8Hz 59
Figure 6.3: Accelerations at 80% fill at frequency 2.8Hz 59
Figure 6.4: Trend line for local maxima of accelerations at 80% fill at frequency 2.8Hz 60
Figure 6.5: Accelerations at 50% and 80% fill at frequency 2.8Hz 60
Figure 6.6: Accelerations at 50% fill at frequency 4.4Hz 61
Figure 6.7: Trend line for local maxima of accelerations at 80% fill at frequency 2.8Hz 61
Figure 6.8: Accelerations at 80% fill at frequency 4.4Hz 62
Figure 6.9: Trend line for local maxima of accelerations at 80% fill at frequency 4.4Hz 62
Figure 6.10: Accelerations at 50% and 80% fill at frequency 4.4Hz 63
Figure 6.11: Accelerations at frequencies 2.8Hz and 4.4Hz at 50% fill 63
Figure 6.12: Accelerations at 50% fill at frequency 2.8Hz 64
Figure 6.13: Trend line for local maxima of accelerations at 50% fill at frequency 2.8Hz 64
Figure 6.14: Accelerations at 80% fill at frequency 2.8Hz 65
Figure 6.15: Trend line for local maxima of accelerations at 80% fill at frequency 2.8Hz 65
Figure 6.16: Accelerations at 50% and 80% fill at frequency 2.8Hz 66
Figure 6.17: Accelerations at 50% fill at frequency 4.4Hz 67
Figure 6.18: Trend line for local maxima of accelerations at 50% fill at frequency 4.4Hz 67
Figure 6.19: Accelerations at 80% fill at frequency 4.4Hz 68
Figure 6.20: Trend line for local maxima of accelerations at 80% fill at frequency 4.4Hz 68
Figure 6.21: Accelerations at 50% and 80% fill at frequency 4.4Hz 69
Figure 6.22: Accelerations at 50% fill at frequency 2.8Hz with and without baffle 70
Figure 6.23: Accelerations at 80% fill at frequency 2.8Hz with and without baffle 70
Figure 6.24: Accelerations at 50% fill at frequency 4.4Hz with and without baffle 71
Figure 6.25: Accelerations at 80% fill at frequency 4.4Hz with and without baffle 71

TABLE OF CONTENTS

TITLE PAGE i
CERTIFICATE ii
ACKNOWLEDGEMENT iii
ABSTRACT iv
LIST OF TABLES v
LIST OF FIGURES vi

1. Introduction 1- 4
   1.1 Introduction 1
   1.2 Background 2
   1.3 Linear Wave Theory 3
   1.4 Fluid-Structure Interaction ……4
   1.5 Free Surface Representation ……4

2. Literature Review 5-16
   2.1 Introduction 5
   2.2 Seismic Performance of Liquid Storage Tanks in Historic Earthquakes 6
      2.2.1 The Great Chilean Earthquake 6
      2.2.2 Imperial Valley Earthquake 7
      2.2.3 The Bhuj (India) Earthquake.....7
      2.2.4 The Great East Japan (Tohoku) Earthquake 8
   2.3 Importance of Sloshing 10
   2.4 Provisions for the Design of Storage tanks …… 11
   2.5 Fluid-Structure Interaction.....13
   2.6 Computational Studies 15
   2.7 Numerical and Experimental Studies ……...16

3. Physical Model 17-20
   3.1 Introduction 17
   3.2 Motion of the Tank 18
      3.2.1 Sinusoidal Motion of the Tank 18
   3.3 Tank with Baffles ……19
   3.4 Objectives ….....20

4. Mathematical Formulation…… 21-30
   4.1 Continuity Equation ……21
   4.2 Navier-Stokes Equation 21
   4.3 Multiphase governing Equations 22
      4.3.1 Conservation of Momentum 22
      4.3.2 Turbulence modeling 22
   4.4 Mathematical Model 23
   4.5 The Equivalent Mechanical System ….....28

5. Experimental Setup and Observations ……31-57
5.1 Instrumentation 31
5.2 Experimental Procedure 32
5.3 Observations 33
5.3.1 The shape of the standing waves at resonance ..……...34
5.3.2 Formation of waves during seismic excitation …..……..38
5.4 Readings Obtained 45

6. Readings and Discussion …….....58-72
6.1 Case 1: When the tank is subjected to seismic excitation of frequency 2.8Hz without baffle.....58

6.2 Case 2: When the tank is subjected to seismic excitation of frequency 4.4Hz without baffle .…….....61
6.3 Case 3: When the tank is subjected to seismic excitation of frequency 2.8Hz and 4.4Hz with baffle height 0.3m 64
6.4 Case 4: When the tank is subjected to seismic excitation of frequency 2.8Hz and 4.4Hz with baffle height 0.4m 67
6.5 Case 5: Comparison of accelerations at natural frequency 2.8Hz with and without baffle at 50% and 80% fill 69
6.6 Case 6: Comparison of accelerations at natural frequency 4.4Hz with and without baffle at 50% and 80% fill 71

7. Conclusions 73-74
7.1 Conclusions 73
7.2 Scope of Future Work ……......74

REFERENCES

CHAPTER 1

INTRODUCTION

1.1 Introduction

Liquid storage tanks are important components of lifeline and industrial facilities. Failure of tanks especially in the case of storing combustible and perilous materials can lead to extensive disasters. Tanks maybe divided into various categories based on their material, shape, support type etc. Several researchers have investigated on liquid storage tanks behavior in static and dynamic conditions considering simplified assumptions and also, features such as fluid-structure interaction and surface sloshing [1].

"Sloshing can be defined as dynamic load acting over a tank structure as a result of the motion of a fluid with free surface confined inside the tank. Liquid sloshing is a kind of wave motion inside a partially filled tank. Under external excitations, with large amplitude or near the natural frequency of sloshing, the liquid inside a partially filled tank is in violent oscillations. In this work we will see the background behind the sloshing phenomena to define the problem in proper manner. Also we will see the research work carried related to this problem, proposed methodology to go for solution and scope of work. Sloshing can be the result of external forces due to acceleration and deceleration of the containment body [2]. The force analysis of the reservoirs or tanks is about the same irrespective of the chemical nature of the product [6]. In road tankers, the free liquid surface may experience large excursions for even very small motions of the container leading to stability problems [12].

Of particular concern is the pressure distribution on the wall of the container reservoir and its local temporal peaks that can reach up to twice its rated capacity during resonance at the time of earthquake.

It is known well that the hydrodynamic load exerted by liquid sloshing can cause severe structural damage. One of the passive devices to control liquid flow and suppress liquid sloshing is the baffle installed inside a tank. Sloshing of liquid in a container is a phenomenon encountered within various industries like chemical, petroleum, offshore, shipping etc.

A free surface, i.e., a boundary between two homogenous fluids such as liquid and air, is required for sloshing to occur. The problem of water sloshing in closed containers is a big problem and has been a topic of studies since a very long time. This phenomenon is occurred due to the sudden change in loads. In order to design the equipment detailed understanding of the liquid under sloshing is required. [11]"

Hence, this project consists of two parts. First part consists of simplified analysis of the total seismic response of rectangular liquid storage tanks at different guiding frequencies to obtain its natural frequencies at different modes. Second part consists of the study to check variation of baffle height relative to different liquid fill levels, affects the sloshing phenomenon, when the tank with vertical baffle at the center of the bottom wall, seismically excited with frequency equal to natural frequency of the liquid in the tank. Two cases of the tank motions are considered, i.e., when the tank is subjected to seismic excitation of natural frequency at second mode and fourth mode. Then for both the above cases liquid filling levels considered are 50% and 80% of the tank depth. Furthermore, two vertical baffles of height 0.3m and 0.4m are inserted on the bottom of the tank to control the impact pressure and then all results are compared to find out the best possible case.

1.2 Background

Liquid sloshing in storage tanks due to earthquakes is of great concern and it can cause various engineering problems and failures of structural system. These damages include: Buckling of ground supported slender tank, rupture of steel tank shell at the location of joints with pipes, collapse of supporting tower of elevated tanks, cracks in the ground supported RC tanks, etc. During Alaska earthquake, many tanks suffered typical damage such as fire, buckling of floating roof caving of fixed roofs and failures on structural systems of tank. In Japan, many petroleum tanks were damaged by the sloshing during 1964 Niigata earthquake, 1983 Nikonkai-chubu earthquake and 2003 Tokachi-oki earthquake. Therefore, the stability of the liquid storage tanks under earthquake conditions must be studied carefully.

1.3 Linear Wave Theory

Linear wave theory is one of the first types of mathematical modeling used to analyze wave motion. It is the core theory of ocean surface waves used in ocean and coastal engineering and naval architecture and generally used to evaluate the seismic response of liquid storage tanks. It provides some insight into wave motion at a relatively simple level. Sloshing is often analyzed in a simpler form where no overturn takes place. Mathematically it is based on the governing equation of continuity and potential flow assumptions. Assumptions like incompressibility, irrotational flow, inviscid (viscous/drag/friction terms are negligible), no ambient velocity (no current), and small amplitudes are also allowed for a simplified analysis via linear wave theory.

Linear wave theory for a 3-D liquid container yields following equation which represents the nth mode oscillation frequency "ω_n" in a container of length "l" and fluid height "h".

$$\omega_n^2 = \frac{n\pi g}{l}\tanh\left(\frac{n\pi h}{l}\right) \tag{1.1}$$

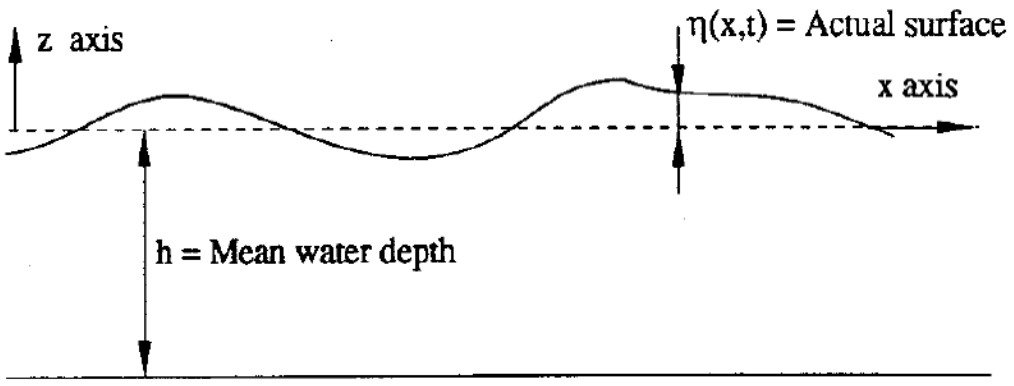

Figure 1.1: Linear Wave Motion[21]

1.4 Fluid structure interaction (FSI)

Fluid-Structure Interaction refers to the coupling of unsteady fluid flow and structural deformation. It is a two-way coupling of pressure and deflection. Its application includes airbag modelling, fuel tank sloshing, heart valve modelling, helicopter crash landings, etc.

Purpose of studying FSI is that fluid mechanics may affect and be affected by the structural mechanics, and vice-versa. Hence in this case the coupling of the fluid's pressure and the motion of the structure is essential.

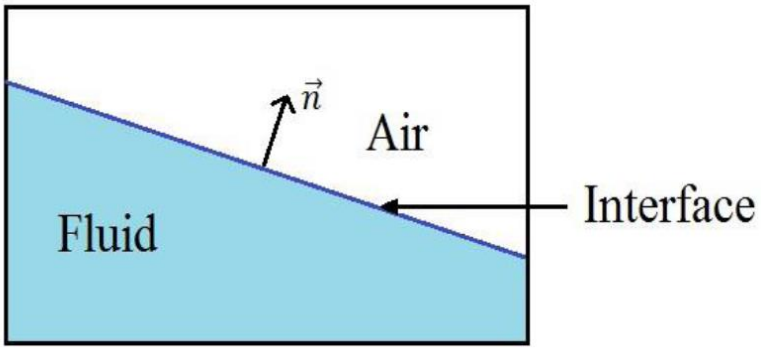

Figure 1.2: Fluid Structure Interaction[6]

1.5 Free surface Representation

Several techniques exist for tracking immiscible interfaces, and these can be classified under three main categories according to physical and mathematical approach:

1. Moving Grid or Lagrangian approach (Capturing).

2. Fixed grid or Eulerian Approach (Tracking).

3. Combined method of Lagrangian and Eulerian.

Lagrangian approach includes moving-mesh, particle-particle scheme and boundary integral method. Eulerian approach can be divided into two main approaches: Surface tracking and Volume tracking. These include front-tracking, volume of method (VOF), Marker and Cell (MAC) method, smoothed particle hydrodynamics, level set methods, and phase field.

CHAPTER 2

LITERATURE REVIEW

2.1 Introduction

Earthquake force is of special importance in design of storage tanks due to volume and weight of such structures. For this reason, seismic analysis of the storage tanks has been considered by many researchers. “One of the oldest researchers is Jacobson who has collected valuable information about seismic analysis of storage tanks (Abaqus Analysis) . After him, other researchers such as Lysmer and Kuhlemeyer (ADF, 2000) , Stein (Chopra, 1995) , Kausel (Epstein, 1976) etc have conducted broad studies on different fields of seismic analysis of tanks and also the soil surrounding the tank and its behaviour at time of seismic modelling have been regarded as an important and relatively unknown factor in the researches for storage tanks. On the other hands, different methods have been presented based on attitude of the designers in two general classes of static and dynamic analysis. In static analysis, earthquake force and its effect are evaluated by a static force. This force is obtained based on coefficients of the code and the related coefficients. In other words, effect of earth motion on the storage tanks is evaluated and simulated with equivalent static force while force applied to the structure is determined due to earth motion resulting from earthquake force based on dynamic reflection of the structure in dynamic analysis method. Dynamic analysis method includes spectrum analysis method and time history analysis method. In dynamic analysis method, effect of earth motion is specified as acceleration spectrum. In time history dynamic analysis method, effect of earth motion is specified as site acceleration time history.” Therefore, time history analysis requires seismic geotechnical studies in the site to determine earth motion for the desired site based on earthquake risk analysis and response of earth. [15].

Traditionally the non linear potential theory and experimentation on scaled models were used to assess the sloshing loads. But the recent approach for analysis of sloshing loads is Computational Fluid Dynamics (CFD) investigated by Goddridge [1] et al. "The results showed that the sloshing natural frequency and the inertia of the system is affected by the fluid level. Potential flow theory has some limitations that is why CFD is now considered as the most viable tool for analysing such fluid dynamics problems [2-5]. Initial work started in the early 1960's with the study of the influence of liquid propellant sloshing on the flight performance of jet propelled vehicles. Chwang & Wang [7] applied nonlinear theory to calculate the pressure force in accelerating rectangular and circular container [11]."

Pressure variation on tank surfaces:

To evaluate the "strength" of sloshing, acceleration of the tank surface with respect to time is plotted. To evaluate effect of baffles, the maximum acceleration on the tank walls at given time is plotted. When there is more sloshing, the tank fluid moves with more velocity and hence has more dynamics pressure. This fluid then exerts this pressure on the tank wall. Due to presence of baffles, the sloshing reduces and hence the dynamic pressure exerted on the tank walls. It is seen that the maximum acceleration of the tank walls is reduced when baffles are used. This shows that the intensity of sloshing has reduced with use of baffles. It's not only the maximum sloshing, but overall sloshing is dampened with usage of baffles.

2.2 Seismic performance of liquid storage tanks in Historic earthquakes

The seismic performance of liquid storing containers is described here under some of the severe historical earthquakes. Also the mechanism leading to their failure is discussed.

2.2.1 The great Chilean earthquake

It was of magnitude 9.5 on 22 may, 1960 is the most powerful earthquake till date. Many storage tanks were severely damaged or failed in this earthquake. This was particularly the case where the support system consisted of vertical columns circumferentially disposed, attached by one or more levels of circumferential beams. Failure due to plastic hinges in beams and columns in the circular frames of support structure was common (Priestley et al., 1986).

2.2.2 Imperial Valley earthquake

It occurred on 15 october, 1979 on Imperial fault near United States-Mexican border. It was of magnitude 6.5 on scale. Two large tanks at Imperial Irrigation District Power plant suffered roof-damage of similar kind. Both tanks were reportedly full at the time of earthquake. The separation of roof from the shell at the roof-shell weld led to the spilling of oil from the tank. Smaller tanks nearby had no significant damage while the largest tank at the site uplifted from the ground. Many other tanks at other sites suffered minor damages which consisted of roof seal damage, broken anti-rotation devices, relief piping damage, grounding cable pull-off, settlement, and strain and swing line damage.

2.2.3 The Bhuj(India) earthquake

The Bhuj, India earthquake of January 26, 2001 measuring 7.7 on magnitude scale damaged many elevated water tanks. Two of them with reinforced concrete (RC) frame staging collapsed while others suffered damage to their staging (support structures). Majority of these tanks, supported on cylindrical shaft staging, developed circumferential flexural cracks near the base (Dutta et al., 2009).

Figure 2.1: Collapsed elevated tank in Bhuj(India)[22]

2.2.4 The Great East Japan(Tohoku) earthquake

It occurred on 11 march, 2011 and its magnitude was 9M. It was followed by tsunami and 5 aftershocks. The oil storage tanks and other hazmat facilities damaged mainly by the Tsunami on the pacific coast and the strong ground motion caused the fire in LPG tank area.

Figure 2.2: Elephant foot buckling of broad tank[22]

Figure 2.3: Diamond buckling in slender tank[17]

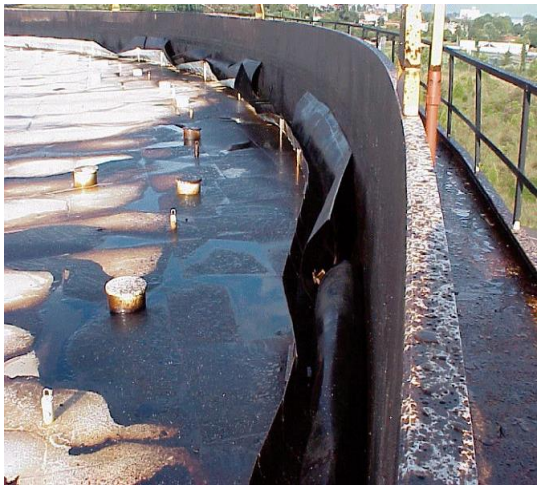

Figure 2.4: Damaged seals in tanks from sloshing of liquids[17]

Figure 2.5: Oil tank sloshing spill over the tank[22]

Figure 2.6: Typical collapsed small steel water tank[22]

2.3 Importance of sloshing

Sloshing is the periodic motion of the free surface of a liquid in partially filled tank or container can be caused by several factors. Sloshing viewed in many industrial applications analysis of the sloshing motion of a contained liquid is of great practical importance. “Motion of a fluid can persist beyond application of a direct load to the container; the inertial load exerted by the fluid is time-dependent and can be greater than the load exerted by a solid of the same mass. This makes analysis of sloshing especially important for transportation and storage tanks. In fact, a significant amount of research has gone into developing numerical models for predicting fluid behavior under various loads. Liquid in an arbitrary shaped container under external excitations, results in surface and bulk turbulence. The nature of such turbulence is quite complex due to several effects such as sloshing, pressure gradient etc. Amongst these, sloshing makes the liquid container more vulnerable to structural damages. Depending on the type of disturbance and container shape, the free liquid surface may experience different types of motion including simple planar, non-planar, rotational, irregular beating, symmetric, asymmetric, quasi-periodic and chaotic. However, the amplitude of slosh depends on the amplitude and frequency of the tank motion, liquid-fill depth, liquid properties and tank geometry.” The resonance in the case of horizontal excitation occurs when the external forcing frequency is close to the natural frequency of the liquid [21].

Hence liquid sloshing is a practical problem with regard to the safety of liquid storage systems during earthquake. Analysis of the sloshing motion of a contained liquid is of great practical importance. Motion of a fluid can persist beyond application of a direct load to the container; the inertial load exerted by the fluid is time-dependent and can be greater than the load exerted by a solid of the same mass. This makes analysis of sloshing especially important for transportation and storage tanks [2].

2.4 Codal Provisions for the design of storage tanks

Indian Standard IS:1893-1984 provides guidelines for earthquake resistant design of several types of structures including liquid storage tanks. This standard is under revision and in the revised form it has been divided into five parts. Thus, for design of structures other than buildings, designer has to refer the provisions of previous version of IS 1893 i.e., IS1893:1984. For seismic design of liquid storage tanks, IS 1893:1984 has very limited provisions. These provisions are only for elevated tanks and ground supported tanks are not considered. Even for elevated tanks, effect of sloshing mode of vibration is not included in IS 1893:1984. Moreover, compared with present international practice for seismic design of tanks, there are many limitations in the provisions of IS 1893:1984. Thus, one finds that at present in India there is no proper Code/Standard for seismic design of liquid storage tanks. It does not consider convective mode. Base shear for elevated tank is given by $V = C_s W$, where, base shear coefficient, C_s is given by

$$C_s = \beta I F_o \frac{Sa}{g} \qquad (2.1)$$

Here, S_a/g = average acceleration coefficient corresponding to the time period of the tank, obtained from acceleration spectra given in the code; F_o = seismic zone factor; W = weight of container along with its content and one third weight of supporting structure. For elevated tanks, Importance factor I = 1.5. It may be noted that in the expression for base shear coefficient of tank, the performance factor K does not appear, i.e. K = 1 is considered, which is same as that for a building with ductile frame. This implies that in IS:1893-1984, there is no provision to account for lower ductility and energy absorbing capacity of elevated tanks. Thus, as per IS:1893-1984, base shear coefficient for tank will be only 1.5 times higher than that for a building, which is due to higher value of importance factor. This is in contrast to other codes, reviewed in earlier sections, wherein tank base shear coefficient is seen to be 3 to 7 times higher than buildings. This lacunae needs to be corrected in the next revision of the code.

Subsequent parts of IS 1893:2002, will be using acceleration spectra given in Part I, and will be based on same design philosophy. Thus, for liquid storage tanks, base shear coefficient will be given by equation 2.2, in which suitable values of R will have to be used for different types of tanks.

$$C_s = \frac{ZI}{2R}\frac{Sa}{g} \qquad (2.2)$$

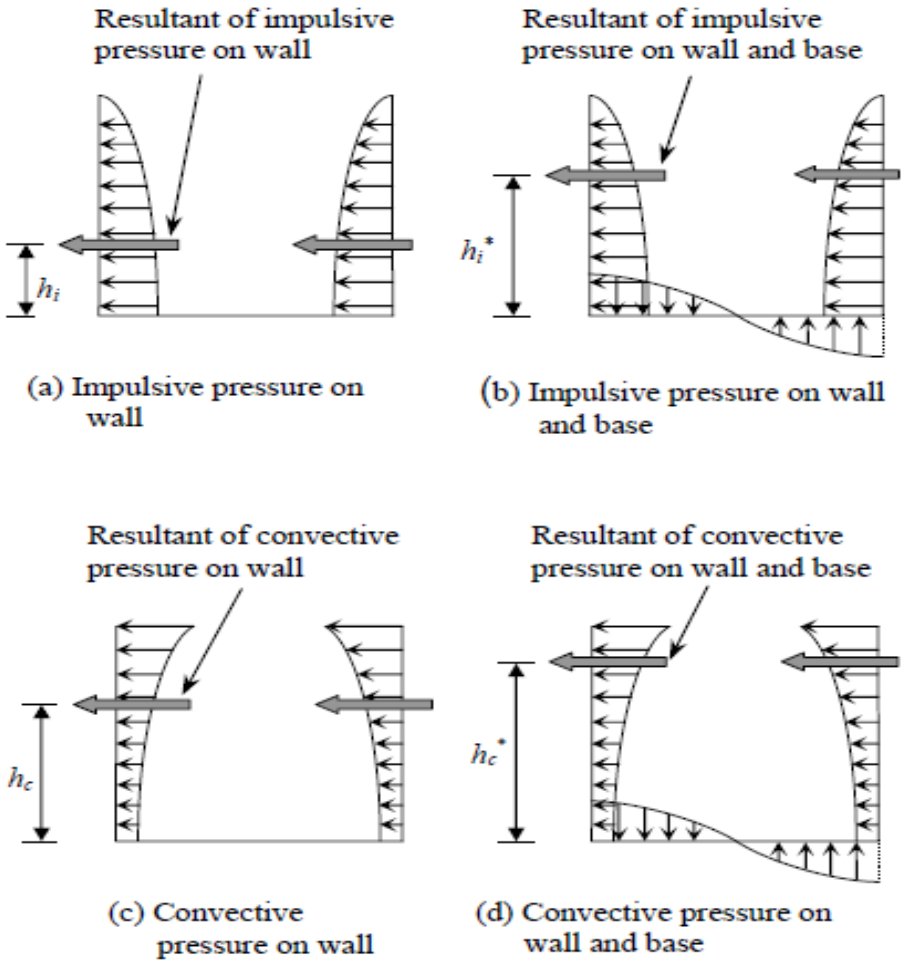

Figure 2.7: Qualitative description of hydrodynamic pressure distribution on tank wall and base[8]

2.5 Fluid-Structure interaction

The response and dynamic behavior of the storage tanks under lateral excitation is generally non-linear in nature and has been studied extensively. The motion of the liquid inside storage tank leads to hydrodynamic pressure loading on the walls of the tank. Housner assumed that the response of the tank can be divided into two hydrodynamic constants as follows:

- Impulsive component: Due to rigid body motion of the liquid. Under dynamic loading a part of the liquid starts moving synchronously with the tank. The liquid acts as an added mass and is subjected to same accelerations as the tank. It is also called rigid-impulsive component.
- Convective component: Due to sloshing at free surface of the liquid. Oscillations of the fluid occur under lateral excitations. This leads to generation of pressure on walls, base and roof of the tank.

Housner derived solutions for the rigid-impulsive and convective pressure components. The rigid-impulsive component of the solution satisfies the actual boundary conditions on the tank walls and base and the condition of zero hydrodynamic pressure at z = H where z is the vertical coordinate (datum is at base of tank) and H is the height of the liquid. The convective component of the solution corrects for the difference between the actual boundary condition at z = H (accounting for the effects of sloshing of the liquid) and the one used in the development of the rigid-impulsive solution.

Following from the solutions, Housner proposed a mechanical (spring-mass) model, as shown in Figure below, for representing the response of the rigid tank-liquid system. The rigid-impulsive mass is assumed to be rigidly attached to the container walls while the convective mass is split into a series of sub-masses $m_1, m_2, \ldots, m_n$ associated with the $1^{st}, 2^{nd}, \ldots, n^{th}$ sloshing masses respectively. These latter masses are attached to the container wall via springs of stiffness $k_1, k_2, \ldots, k_n$ representing the $1^{st}, 2^{nd}, \ldots, n^{th}$ anti-symmetric sloshing frequencies respectively.

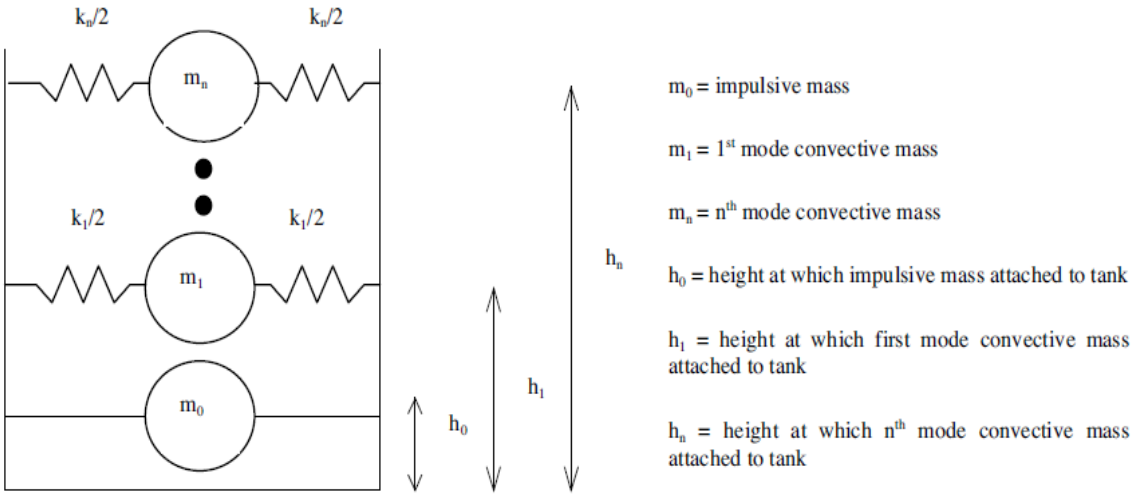

Figure 2.8: Housner's mechanical spring model for tanks[19]

When a storage tank is subjected to lateral excitations then sloshing takes place and pressure is exerted on the walls and base of the tank. This sloshing is described by an infinite number of anti-symmetric modes with the first four modes for a typical tank model as shown below:

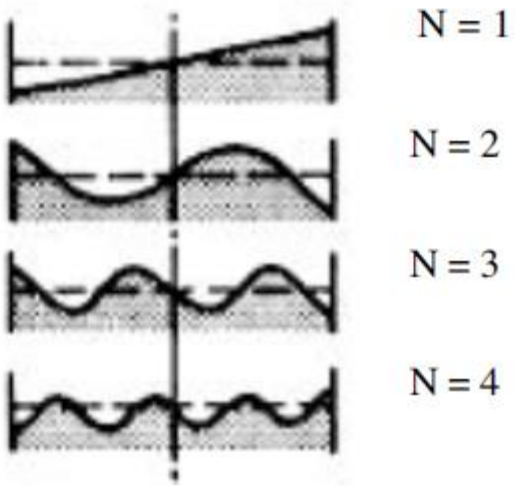

Figure 2.9: Anti-symmetric modes for rectangular tanks[19]

2.6 Computational Studies

Ling Hou et al. [1] studied sloshing performance in a 2-D rectangular tank. In this study, transient analysis is performed under single and multiple-coupled external excitations for two different frequencies using ANSYS-FLUENT software. Volume of fluid (VOF) method was used to track the free surface of liquid and dynamic mesh technique to impose external excitation. The result shows that at coupled excitations and near resonant excitation frequencies, sloshing behavior will become violent and sloshing loads, including impact on the top wall, will be intensified.

J.H. Jung et al. [2] investigated the effect of the vertical baffle heights on the liquid sloshing in a three-dimensional (3D) rectangular tank with 70% water fill level. He selected various ratios of baffle height (hB) to initial liquid height(h).For simulation of 3D incompressible, viscous, two-phase flow in a tank partially filled with liquid and equipped with baffles, the volume of fluid (VOF) method based on the finite volume method has been used. Result shows that after a certain height (critical height) of baffle, the liquid does not reach at roof top and when baffle height is greater than liquid fill level.

Vaibhav singal et al. [3] studied sloshing phenomenon in a partially filled kerosene tank using volume of fluid (VOF) multiphase model with and without the use of baffles. Computational study was done using Finite volume method in ANSYS-FLUENT software. Result shows that sloshing in the fuel tank was effectively reduced with the use of baffles in the tank.

Krit Threepopnartkul et al .[4] studied the effect of baffles on reducing severe sloshing inside moving rectangular tank. He used Finite volume method for analyzing fluid sloshing in tank. Computational models were used to investigate effects of baffles. This study has been done using C++ codes implemented in the Open Source software. The whole simulation was done experimentally as well as computationally and both the results were digitized using the image processing techniques having the average error less than 3.73%.

S. Rakheja et al. [5] studied effectiveness of different design of baffle, including lateral, oblique, conventional and partial under longitudinal and lateral acceleration for different fill levels in a 3-D truck tank. The result shows that the conventional lateral baffles are more effective to fluid slosh under longitudinal acceleration only while the oblique baffle helps to reduce both longitudinal as well as lateral slosh forces.

2.7 Numerical and Experimental studies

Lyes Khezzar et al. [12] done experimental study on a test rig (560 x 160 x 185 mm rectangular container) to study water sloshing phenomenon subjected to sudden (impulsive) impact. Motion of fluid was recorded using a video camera. Two water fill levels of 50 and 75% with two driving weights of 2.5 and 4.5 kg were used. Finally, flow fields, obtained using the numerical code were compared with experimental results.

Dongming Liu et al. [13] developed a numerical model for liquid sloshing in a 3-D tank with baffles. The spatially averaged Navier–Stokes equations were solved numerically. The large-eddy-simulation (LES) approach is used to model turbulence by using the Smagorinsky sub-grid scale (SGS) closure model. The baffles are modeled by virtual boundary force (VBF) method. The numerical model is validated against the analytical solution and experimental data for 2-D as well as 3-D liquid sloshing in a tank with and without baffles.

Mi-An Xue et al. [14] numerically solved Navier-Stokes equations for investigation of liquid sloshing phenomenon in a cubic tank with various configurations of horizontal baffle, perforated vertical baffle, and their combined configurations under the harmonic motion excitation. Experimental testing of liquid sloshing in cubic tank with perforated vertical baffle was simulated to validate numerical results.

Y.G. Chen et al. [15] simulated sloshing in a partially filled tank excited by dynamic load to calculate the impact pressure. For free surface representation, Reynolds-averaged Navier–Stokes (RANS) is used which a two-fluid approach based on a level set method. For numerically investigation purpose, rectangular tank was excited by horizontal harmonic motion and harmonic rolling motion. The computed results were compared with experimental data and show that simulation of dynamic pressure loads exerted on the tank walls and ceiling can be done very effectively with numerical methods.

M. A. Goudarzi et al. [16] analytically estimated hydrodynamic damping ratio for liquid sloshing phenomenon in a partially filled rectangular tank for baffles. They used the velocity potential formulation and linear wave theory for analytic calculations. For validation of analytically obtained results, they experimentally excited the rectangular tank with harmonic oscillation frequencies and results were compared. Different baffle configuration (both vertical and horizontal) at different locations and dimensions are studied to analyze their damping efficiencies.

CHAPTER 3

PHYSICAL MODEL

3.1 Introduction

The physical model used for present study is shown in figure. Present model consists of a 3-dimensional liquid storage rectangular tank which is partially filled with water (ρ=999.98 kg/m3, μ=0.00103 kg/m-s). The tank dimensions are 0.3*0.3*0.6 m^3. The rectangular walls are made up of Perspex plates housed inside a steel frame. It has a density of 1.17–1.20 g/cm^3, which is less than half that of glass. Water fill level in tank is 50% and 80% of total height of tank and the rest part is occupied with air.

During the seismic excitation mode, tank is supposed to go under sloshing effect which creates pressure and forces on tank wall. During computation, pressure is monitored at a certain points on the left wall in order to record the sloshing loads. To reduce the effect of sloshing on tank wall, tank is equipped with vertical baffle of thickness 0.5cm and of different height which depends on fill level of water inside tank. The details of various dimensions of physical model are presented in figure.

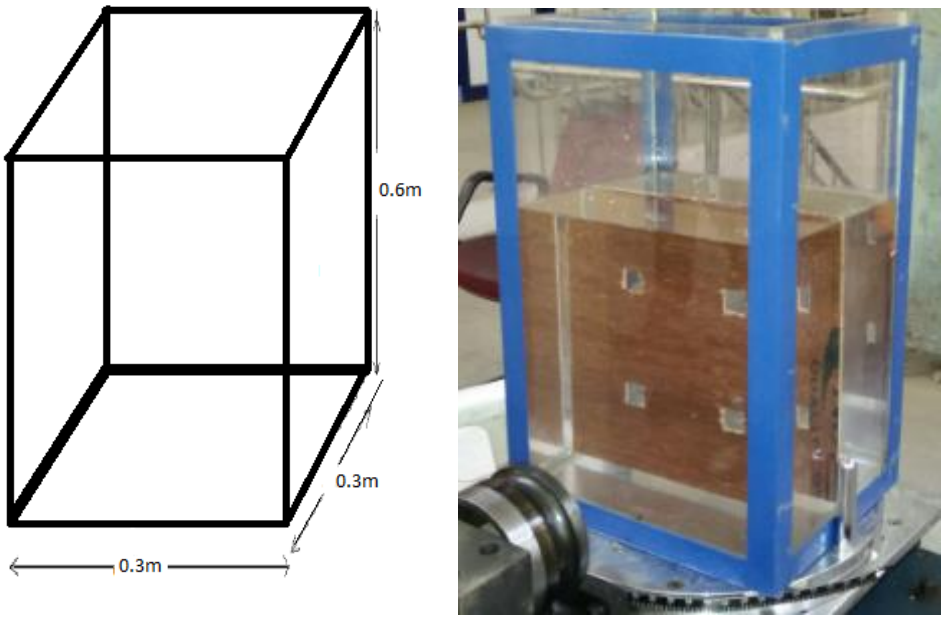

(a) (b)

Figure 3.1: Water tank model

3.2 Motion of the tank

The study has been done for two different cases of seismic excitation frequency at second and third mode:

i. When the storage tank is subjected to seismic excitation of natural frequency at second mode i.e. f =2.8Hz for 50% fill and 80% fill water level, with and without baffle.

ii. When the storage tank is subjected to seismic excitation of natural frequency at fourth mode i.e. f =4.4Hz for 50% fill and 80% fill water level, with and without baffle.

3.2.1 Sinusoidal motion of tank

The motion of the rectangular tank is purely based on sinusoidal base excitation. The tank is excited with an amplitude of 2cm. Motion of the tank can be represented by:

$$\left.\begin{aligned} x &= A\sin(\omega t) \\ \dot{x} &= A\omega\cos(\omega t) \\ \ddot{x} &= -A\omega^2\sin(\omega t) \end{aligned}\right\} \tag{3.1}$$

Where is displacement x, $\dot{x}$ is horizontal translational velocity, $\ddot{x}$ is horizontal acceleration, A is the horizontal displacement amplitude, ω is the angular frequency and t is time period of oscillation.

3.3 Tank with baffles

Sloshing occurs due to motion of fluid inside partially filled tank. So to reduce the severe effect of sloshing baffles are introduced in tank at appropriate locations. In the present study, simulation is done with and without baffle and studied the effectiveness of different height of baffle on sloshing forces and pressures exerted on tank wall. The baffle of thickness 5mm is included at the centre of the tank vertically parallel to YZ plane.

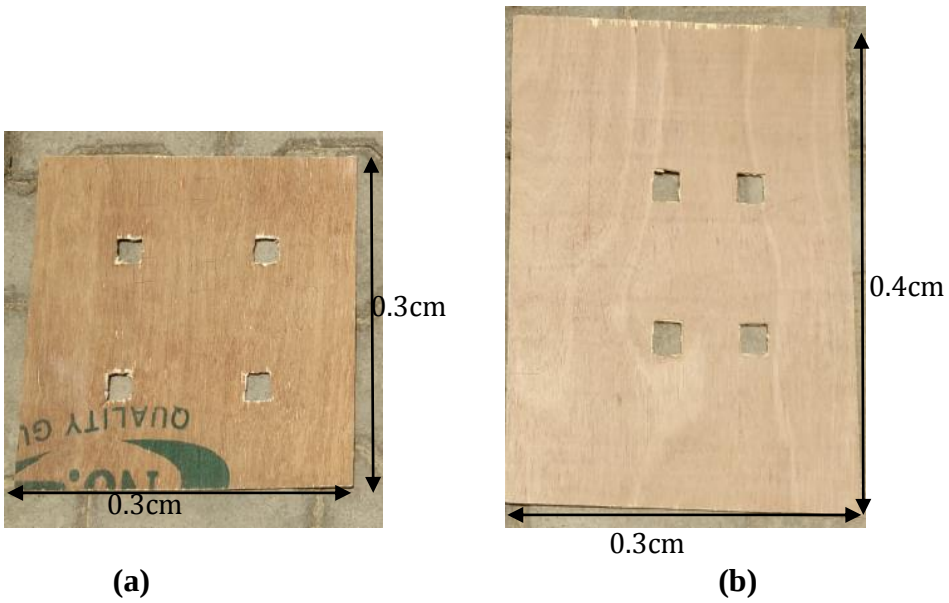

Figure 3.2: Geometry of the baffles used

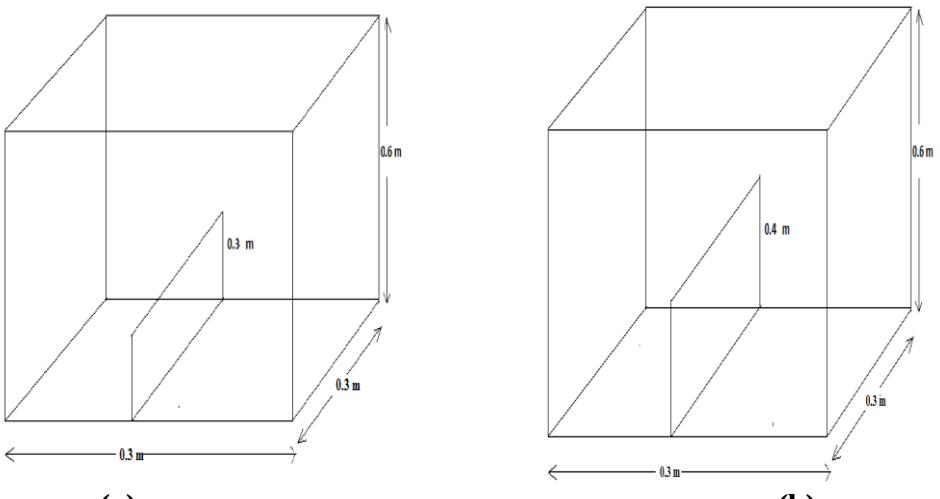

Figure 3.3: Geometry of the tank with baffle

3.4 Objectives

Following are the objectives of this study:

1) Use of a mathematical model based on fluid mechanics background to theoretically predict various frequencies and the wave patterns.
2) Excitation of the liquid volume inside the tank at such frequencies and detection of the frequencies at which standing waves are formed on the liquid surface.
3) To study variation of acceleration values for different parameters on OROS NVGate software and shake table setup and compare with these values.
4) To study the concept of liquid sloshing.
5) To study the effect of slosh forces on stability and structural performance of liquid storage tanks with the help of literature survey.
6) To study the effectiveness of vertical baffles for reducing slosh forces.
7) To study various aspects related to sloshing frequency of liquid in tank, hydrodynamic pressure on wall and analysis of fluid-tank interaction under seismic excitations with the help of literature survey.
8) To study sloshing of water for different baffle heights.
9) To study sloshing of water for different water fill levels.
10) To study water sloshing behavior for various frequency conditions.
11) To compile and analyze the results and to draw conclusions.

CHAPTER 4

MATHEMATICAL FORMULATION

This chapter includes the details of mathematical modeling and solution methods that are generally used for study of sloshing. The mathematical equations describe the flow of liquid in case of sloshing including the motion of the free surface. It is the representation of physical event through mathematical equations. Since the physical events are difficult to model exactly, these equations provide an exact representation of reality. Computational Fluid Dynamics (CFD) techniques are used to solve the governing equation of sloshing numerically. The equations which are used to study sloshing here are: Continuity equation and Navier-stokes equation.

4.1 Continuity Equation

Continuity equation used to describe the transport of conserved quantity. It also defines the conservation of mass.
For 3-dimensional continuity equation for unsteady flow is as follow:

$$\frac{\partial \rho}{\partial t}+\frac{\partial(\rho u)}{\partial x}+\frac{\partial(\rho v)}{\partial y}+\frac{\partial(\rho w)}{\partial z}=0 \tag{4.1}$$

where "ρ" is the density, "*t* " is time, and *u*, *v*, *w* are velocity components in *x*, *y*, *z* direction.
For incompressible and steady flow, continuity equation can be written as:

$$\frac{\partial u}{\partial x}+\frac{\partial v}{\partial y}+\frac{\partial w}{\partial z}=0 \tag{4.2}$$

4.2 Navier-Stokes Equation

Navier-Stokes equations describe the relation between velocity, pressure, temperature, viscosity and density of a moving fluid. This equation is valid for turbulent as well as laminar flow.

$$\frac{\partial(\rho u)}{\partial t}+\rho\left(u\frac{\partial u}{\partial x}+v\frac{\partial u}{\partial y}+w\frac{\partial u}{\partial z}\right)=\rho x-\frac{\partial p}{\partial x}+\frac{1}{3}\mu\frac{\partial}{\partial x}\left(\frac{\partial u}{\partial x}+\frac{\partial v}{\partial y}+\frac{\partial w}{\partial z}\right)+\mu\nabla^2 u \tag{4.3}$$

4.3 Multiphase governing equations

4.3.1 Conservation of momentum

The momentum equation is dependent on the volume fractions of all phases through the properties ρ and μ .

$$\frac{\partial}{\partial t}\left(\rho\vec{V}\right)+\nabla.\left(\rho\vec{V}\vec{V}\right)=-\nabla p+\nabla.\left(\vec{\tau}\right)+\rho\vec{g}+\vec{F} \tag{4.4}$$

where "ρ" is the density, "*t*" is time, "*p*" is the static pressure, μ is dynamic viscosity, τ is the stress tensor, ρ*g* and ρV are the gravitational body force and external body force respectively. F is used here for user-defined source terms, e.g. momentum source which is product of the density of a specific mesh cell and the instantaneous acceleration having units of kg/m^2s^2. Momentum source terms are as follows:

$$\left.\begin{aligned}\vec{F}&=\rho*Acceleration\\ \vec{F}&=\rho*A\omega^2\sin(\omega t)\end{aligned}\right\} \tag{4.5}$$

The stress tensor is as follows:

$$\vec{\tau}=\mu\left[\left(\nabla\vec{V}+\nabla\vec{V}\right)-\frac{2}{3}\nabla.\vec{V}I\right] \tag{4.6}$$

Where is dynamic viscosity, τ is the stress tensor, I is the unit tensor, and term after negative sign is an effect due to volume dilation (size change).

4.3.2 Turbulence modeling

To consider the effect of turbulence fluctuations time-average of Navier-stokes equation should be taken, which is known as Reynolds-Averaged Navier-Stokes equation. In present study we consider k -ε turbulence model which assumes the relation between Reynolds stresses in the fluid and mean velocity gradients.

The turbulence viscosity can be determined by following equation:

$$\mu_t=\rho C_\mu\frac{k^2}{\varepsilon} \tag{4.7}$$

where k is turbulent kinetic energy, μ_t is turbulence viscosity, C_μ is constant of proportionality.

(a) **(b)**

Figure 4.1: Liquid sloshing in membrane tank without baffle[4]

(a) **(b)**

Figure 4.2: Liquid sloshing in membrane tank with baffle[4]

4.4 Mathematical model

Figure 4.3 shows a two-dimensional water tank of length 2*l* containing water up to a height h. We assume that the liquid flow is inviscid, irrorational, and incompressible. We now consider the question as to what type of steady state waves may exist on the liquid surface. We use the notation $\phi(x, y, t)$, $u(x, y, t)$, & $v(x, y, t)$ to represent, respectively, the velocity potential, velocity components in x and y directions. The following equation is known to govern the velocity potential (see, for example, L G Currie, 1974, Fundamentals of mechanics of fluids, McGraw-Hill, NY, pp. 201-205)

$$\frac{\partial^2 \phi}{\partial x^2} + \frac{\partial^2 \phi}{\partial y^2} = 0 \tag{4.8}$$

with the boundary conditions given by-

$$\frac{\partial^2\phi}{\partial t^2}(x,h,t)+g\frac{\partial\phi}{\partial y}(x,h,t)=0$$
$$\frac{\partial\phi}{\partial y}(x,o,t)=0$$
$$\frac{\partial\phi}{\partial x}(\pm l,y,t)=0 \qquad (4.9)$$

The first of the above boundary conditions is obtained by applying the Bernoulli's equation on the free surface and the remaining set of boundary conditions reflects the fact that the normal fluid velocity components at the wall boundaries are zero. The symbol *g* in the above equation represents the acceleration due to gravity and the other notations are explained in figure 4.3. We seek a steady state wave solution of the form-

$$\phi(x,y,t)=\psi(x,y)\cos\omega t \qquad (4.10)$$

This leads to the field equation,

$$\frac{\partial^2\psi}{\partial x^2}+\frac{\partial^2\psi}{\partial y^2}=0 \qquad (4.11)$$

with the boundary conditions-

$$-\omega^2\psi(x,h)+g\frac{\partial\psi}{\partial y}(x,h)=0$$
$$\frac{\partial\psi}{\partial y}(x,o)=0$$
$$\frac{\partial\psi}{\partial x}(\pm l,y)=0 \qquad (4.12)$$

We seek the solution of equation in the variable separable form as $\psi(x, y) = X(x)Y(y)$.

This leads to the equation,

$$\frac{d^2X}{dx^2}Y+X\frac{d^2Y}{dy^2}=0 \qquad (4.13)$$

Dividing both sides by XY one gets,

$$\frac{1}{X}\frac{d^2X}{dx^2}=-\frac{1}{Y}\frac{d^2Y}{dy^2}=-\lambda^2 \text{ (say)} \qquad (4.14)$$

This leads to,

$$\frac{d^2X}{dx^2} + \lambda^2 X = 0$$
$$\frac{d^2Y}{dy^2} - \lambda^2 Y = 0 \qquad (4.15)$$

with boundary conditions:

$$\frac{dX}{dx}(\pm l) = 0; \quad \frac{dY}{dy}(0) = 0; \quad g\frac{dY}{dy}(h) - \omega^2 y(h) = 0 \qquad (4.16)$$

From the first equation of (4.15), one gets

$$X(x) = a\cos\lambda x + b\sin\lambda x \qquad (4.17)$$

Imposing the first boundary condition of equation (4.16), we will get

$$\lambda\begin{bmatrix} -\sin\lambda l & \cos\lambda l \\ \sin\lambda l & \cos\lambda l \end{bmatrix}\begin{Bmatrix} a \\ b \end{Bmatrix} = 0 \qquad (4.18)$$

For nontrivial solution, we will get the condition: $\lambda \sin\lambda l \cos\lambda l = 0$

This leads to two families of solutions, namely,

$$\lambda_n = \frac{n\pi}{l}; n = 1,2,3,\ldots,\infty$$
$$\lambda_m = \frac{(2m+1)\pi}{2l}; m = 0,1,2,3,\ldots,\infty \qquad (4.19)$$

Considering now the second equation of (4.15), we will get

$$\frac{dY}{dy}(0) = 0 \Rightarrow d\lambda = 0 \Rightarrow d = 0$$
$$g\frac{dY}{dy}(h) - \omega^2 y(h) = 0 \Rightarrow g\lambda\sinh\lambda h - \omega^2\cosh\lambda h = 0$$

And, $\omega^2 = g\lambda\tanh\lambda h$ (4.20)

Thus, Combining equation (4.19) and (4.20), we will get

$$\omega_n^2 = \frac{n\pi}{l} g \tanh\left(\frac{n\pi h}{l}\right); n = 1,2,\ldots,\infty$$
$$\omega_m^2 = \frac{(2m+1)\pi}{2l} g \tanh\left(\frac{(2m+1)\pi h}{2l}\right); m = 0,1,2,\ldots,\infty \quad (4.21)$$

This leads to two families of standing wave patterns:

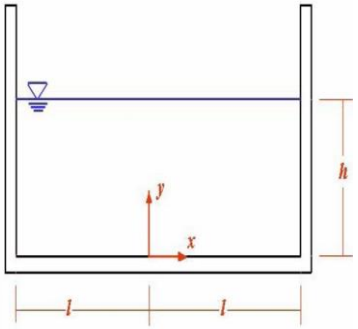

Figure 4.3: Geometry of water stored in rectangular tank

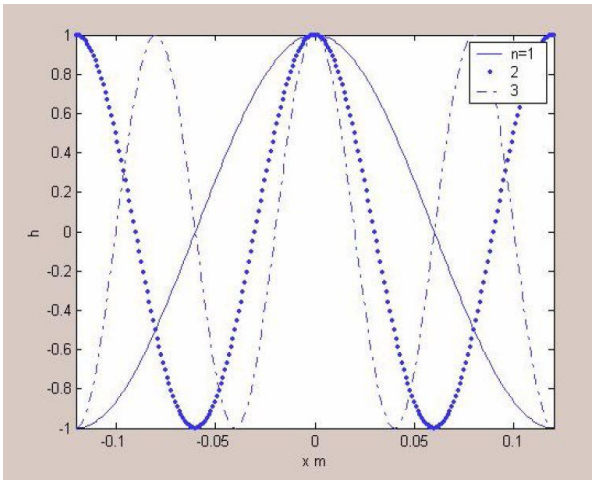

(a)

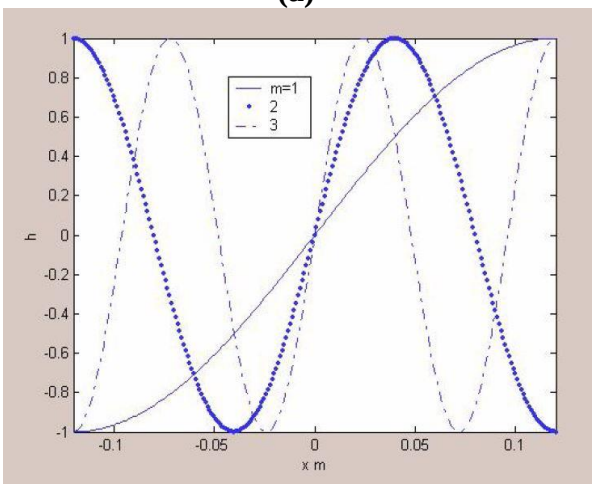

(b)

Figure 4.4: The first few modes of oscillations of the liquid surface estimated using theory[25]

Theoretical Calculations:

To get the theoretical values of natural frequencies, referring equation (4.21),

$$\omega_n^2 = \frac{n\pi}{l} g \tanh\left(\frac{n\pi h}{l}\right); n = 1,2,\ldots,\infty$$
$$\omega_m^2 = \frac{(2m+1)\pi}{2l} g \tanh\left(\frac{(2m+1)\pi h}{2l}\right); m = 0,1,2,\ldots,\infty \quad (4.22)$$

And, $f = \frac{w}{2\pi}$

In our case, total length of tank = 0.3 m

i.e., l = 0.15 m

and, h = 0.2 m, g = 9.81 m/s^2

substituting these values in equation (4.22) for n = 1,2,3,……,∞ and m = 0,1,2,3,……,∞ to get two sets of solution for natural frequencies. Then we will get,

For, n = 1; w_{n1} = 205.36 rad/s thus, f_{n1} = 2.28 Hz

n = 2; w_{n2} = 410.92 rad/s f_{n2} = 3.23 Hz

n = 3; w_{n3} = 616.38 rad/s f_{n3} = 3.95 Hz

Similarly for, m = 0; w_{m1} = 99.66 rad/s thus, f_{m1} = 1.56 Hz

m = 1; w_{m2} = 308.19 rad/s f_{m2} = 2.78 Hz

m = 2; w_{m3} = 513.65 rad/s f_{m3} = 3.61 Hz

m = 3; w_{m4} = 719.11 rad/s f_{m4} = 4.27 Hz

4.5 The equivalent mechanical system

Reducing the fluid system to one of simple oscillators it became possible to investigate the areas of applicability of Housner's theory.

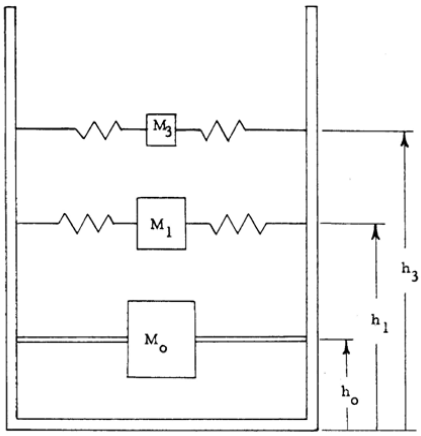

Figure 4.5: Equivalent mechanical system of simple oscillators[5]

To measure the forces acting on the walls of the storage tank a mechanical system as shown in the figure below was studied and experiments were designed to approach this idealisation.

The following notation will be used while analysing the mechanical system:

M_1 = Equivalent oscillating mass of first mode

M_R = The total rigid mass of the system

M_o = The eqivalent rigid mass of impulsive forces

M_o^h = The rigid mass of the fluid below depth h

K_1 = The equivalent spring constant of mass M_1

K_2 = The equivalent constant of the mounting springs

X_1 = Displacement of M_1 relative to the tank walls

X_o = Displacement of M_o relative to the base

V = Potential Energy

T = Kinetic Energy

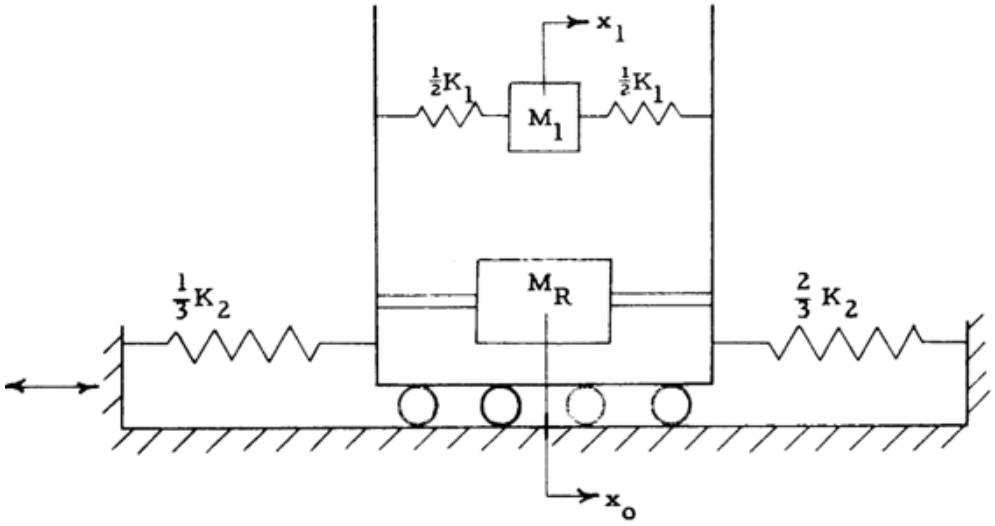

Figure 4.6: Equivalent mechanical system considering the first mode of osscilation[5]

A_o = Amplitude of tank relative base

A_1 = Amplitude of mass M_1 , relative to the container walls

$A_i^{(r)}$ = Amplitude of mass M_i , in the r^{th} principal mode

The expressions for the potentialenergy, V, and for the kinetic energy, T, are

$$V = \tfrac{1}{2} K_1 x_1^2 + \tfrac{1}{2} K_2 x_o^2$$

$$T = \tfrac{1}{2} M_R \dot{x}_o^2 + \tfrac{1}{2} M_1 (\dot{x}_1 + \dot{x}_o)^2 \qquad (4.23)$$

Using Lagrange's equation,

$$\frac{\partial}{\partial t} \frac{\partial T}{\partial \dot{x}_i} - \frac{\partial T}{\partial x_i} + \frac{\partial V}{\partial x_i} = 0, \qquad (4.24)$$

The equations of motion of the system are

$$(M_R + M_1) \ddot{x}_o + M_1 \ddot{x}_1 + K_2 x_o = 0$$

$$M_1 \ddot{x}_o + M_1 \ddot{x}_1 + K_1 x_1 = 0 \qquad (4.25)$$

To simplify the notations are modified as follows:

$$K_{00} = K_2 \qquad M_{00} = (M_R + M_1)$$

$$K_{11} = K_1 \qquad M_{11} = M_1$$

Thus the equations become

$$M_{00}\ddot{x}_0 + M_{11}\ddot{x}_1 + K_{00}x_0 = 0$$
$$M_{11}\ddot{x}_0 + M_{11}x_1 + K_{11}x_1 = 0 \tag{4.26}$$

In order to determine the natural frequency of the system a harmonic solution is assumed

$$x_i = A_i \sin(\omega t + \beta) \tag{4.27}$$

and it substituted in equation 4.11 to obtain the following set of equations:

$$(K_{00} - M_{00}\omega^2) A_0 + (-M_{11}\omega^2) A_1 = 0$$
$$(-M_{11}\omega^2) A_0 + (K_{11} - M_{11}\omega^2) A_1 = 0 \tag{4.28}$$

For a non-trivial solution the determinant of the cofficients must be set equal to zero and obtain the natural frequency equation

$$\omega^4 - \omega^2 \left[\frac{(M_{00}K_{11} + K_{00}M_{11})}{(M_{00}M_{11} - M_{11}^2)} \right] + \frac{K_{00}K_{11}}{(M_{00}M_{11} - M_{11}^2)} = 0 \tag{4.29}$$

Here the values of natural frequrncy can be calculated by setting the initial values and finding the constants. The general solution for the above equation is

$$x_i = \sum_{r=1}^{n} A_i^{(r)} \sin(\omega_r t + \beta_r) \tag{4.30}$$

Where r corresponds to the mode being considered and i to the coordinate.

CHAPTER 5

EXPERIMENTAL SETUP AND OBSERVATIONS

The figure 5.1 shown below provides complete setup used for the experimental study. It consists of (a) shake table , (b)oscilloscope , (c)amplifier and (d) tank model. Here the vibrations from the motor are transferred to the shake table through the (e) shaft. Frequency of excitation can be changed with the help of a knob and it can be seen on the digital display provided.

5.1 Instrumentation

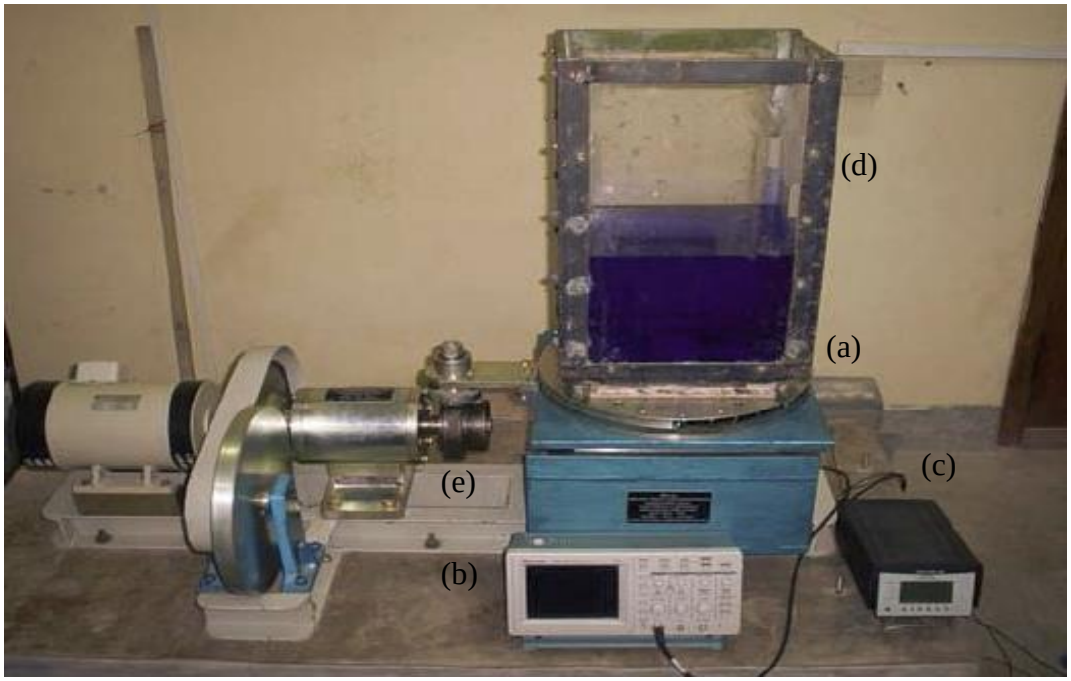

Figure 5.1: Experimental setup

Table 5.1: Equipments used in conducting experiment on water tank

No.	Equipments	Quantity
1	Oscilloscope	1
2	Accelerometers	3
3	Signal conditioning amplifier	1
4	Shake table	1
5	Baffles	2

5.2 Experimental Procedure

1. We mounted the water tank on the shake table as shown in figure 5.1 . List of equipment and sensors needed to perform this experiment is given in table 5.1.
2. Then we measured the dimensions of the tank and the water level inside the tank. A color dye was added to the water so as to facilitate visual observations of the water surface oscillations.
3. Then the tank was excited harmonically starting with low values of frequency. At each frequency the behavior of the water surface was observed visually.
4. At every value of the frequency sufficient time was allowed to pass so that oscillations of water could reach steady state.
5. As the frequency of driving approaches one of the natural frequencies, the water surface begin to oscillate with perceptible amplitudes (figure 5.2). The frequency at which such oscillations occur were noted down. The observations were recorded as given in Tables 6.1.
6. The shape of the standing waves at the liquid surface for first few modes can be observed clearly.
7. The frequencies and shapes of the standing waves using the theoretical formulation provided in section 4.4 were calculated.
8. The theoretical and experimental results are compared in chapter 6 and conclusions are drawn on their mutual agreement/disagreement.
9. The experiment was then repeated for different values of heights of water level inside the tank and readings were taken from the software and recorded in excel.
10. Then the study has been done for the following cases of seismic excitation frequency as obtained above.

i. When the storage tank is subjected to seismic excitation of natural frequency at second mode i.e. fn =2.8Hz for 50% fill and 80% fill water level. And at these two fill levels further cases are considered i.e. tank with and without baffles.

ii. When the storage tank is subjected to seismic excitation of natural frequency at fourth mode i.e. fn =4.4Hz for 50% fill and 80% fill water level. . And at these two fill levels further cases are considered i.e. tank with and without baffles.

5.3 Observations

In first part of this study the phenomena of formation of standing waves on free surface of liquid inside a rectangular container is studies. The setup used for this purpose is shown in figure 5.2. This consists of a rectangular tank whose walls are made up of Perspex plates housed inside a steel cage.

The tank is mounted on an electro-mechanical shake table that supplies harmonic base motions to the tank base. This motion can be viewed, to a first approximation, as the earthquake induced motions on a rectangular tank mounted directly on the ground.

We have recorded the complete process with the help of camera. The vibration patterns of the liquid free surface can be clearly identified in those videos. In this section we have tried to show the wave patterns formed at different frequencies. These pictures are the screenshots taken from the videos so as to analyze the phenomenon accurately.

5.3.1 The shape of the standing waves at resonance at the liquid surface for first few modes are as follows:

From the first part of this study it is observed that first mode of vibration of the tank occurs at 1.6Hz. It is clearly visible that the setup reaches resonance at 1.6Hz because movement of the tank becomes vigorous and sloshing height is considerably increased.

Figure 5.2: Surface profile at first mode (f_n= 1.6Hz)

The second mode, third mode and fourth mode of vibration of the tank occur at excitation frequencies of 2.8Hz, 3.7Hz and 4.4Hz respectively . A standing wave is formed at the free surface of the liquid which is similar to those predicted by the theoretical analysis done in section 4.4. These wave pattern formed at different modes can be clearly seen in figure 5.3, 5.4 and 5.5.

Figure 5.3: Surface profile at second mode (f_n= 2.8Hz)

Figure 5.4: Surface profile at third mode (f_n= 3.7Hz)

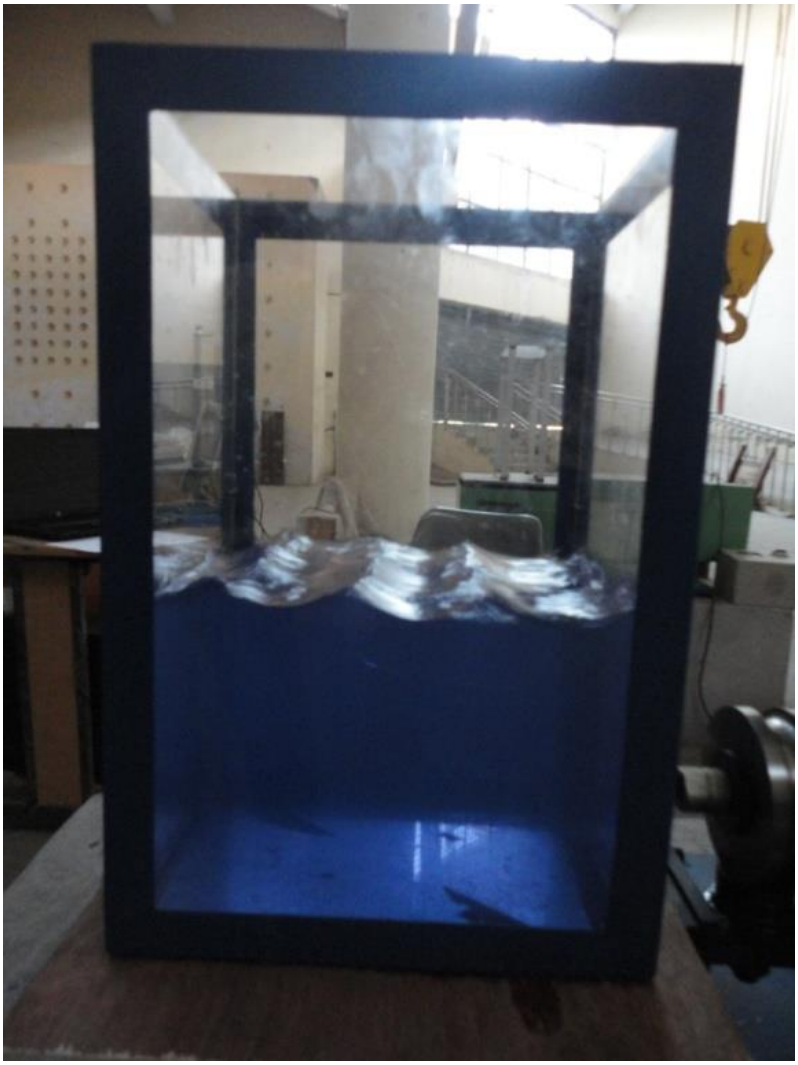

Figure 5.5: Surface profile at fourth mode (f_n= 4.4Hz)

5.3.2 Formation of waves during seismic excitation at first and second mode, with and without baffle:

Second part of this study is done by taking the frequencies of second and fourth mode into account. This is done to see the effect of baffles at two different modes. Figure 5.6 shows the surface profile of the liquid free surface when the tank is provided with 0.3m high baffle and is seismically excited with 2.8Hz frequency. In this case the tank fill level is 50%.

Figure 5.6: Surface profile at 50% fill at frequency 2.8Hz with baffle height 0.3m

Figure 5.7 shows the surface profile of the liquid free surface when the tank is provided with 0.3m high baffle and is seismically excited with 4.4Hz frequency. In this case the tank fill level is 50%.

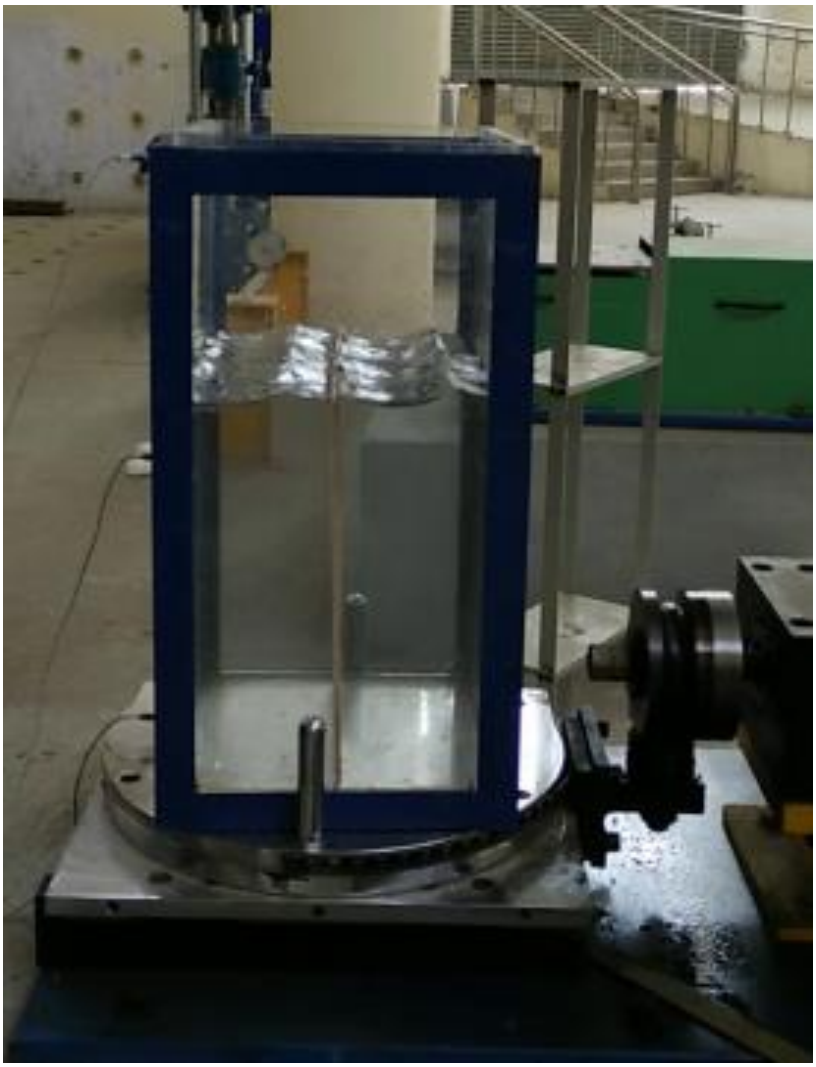

Figure 5.7: Surface profile at 50% fill at frequency 4.4Hz with baffle height 0.3m

Figure 5.8 shows the surface profile of the liquid free surface when the tank is provided with 0.3m high baffle and is seismically excited with 2.8Hz frequency. In this case the tank fill level is 50%.

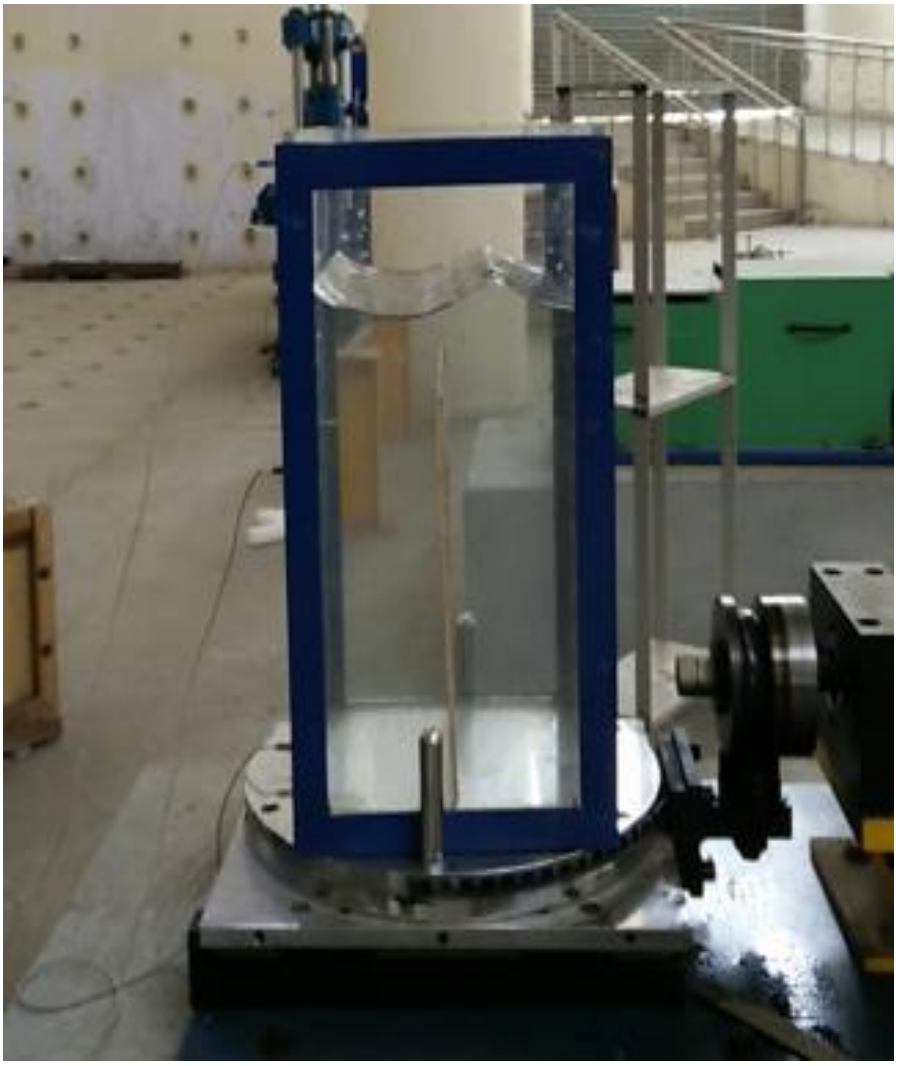

Figure 5.8: Surface profile at 80% fill at frequency 2.8Hz with baffle height 0.3m

Figure 5.9 shows the surface profile of the liquid free surface when the tank is provided with 0.4m high baffle and is seismically excited with 2.8Hz frequency. In this case the tank fill level is 80%.

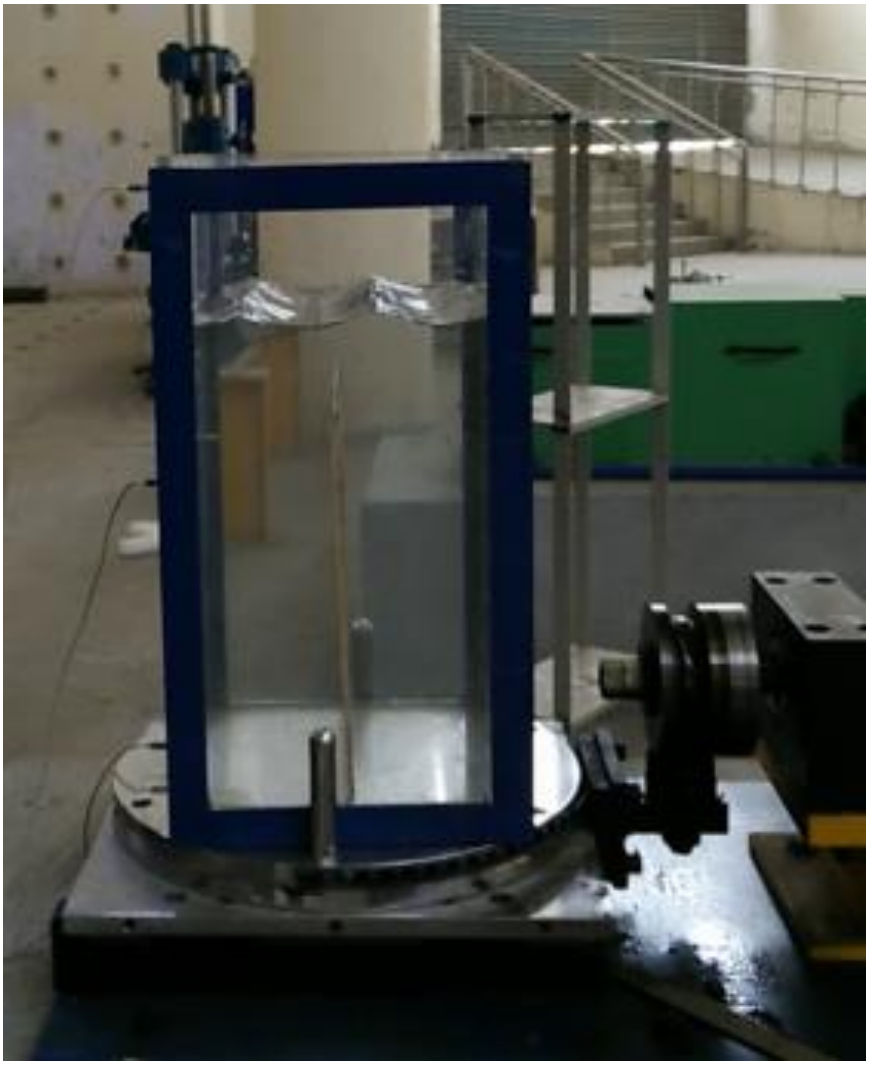

Figure 5.9: Surface profile at 80% fill at frequency 2.8Hz with baffle height 0.4m

Figure 5.10 shows the surface profile of the liquid free surface when the tank is provided with 0.4m high baffle and is seismically excited with 4.4Hz frequency. In this case the tank fill level is 80%.

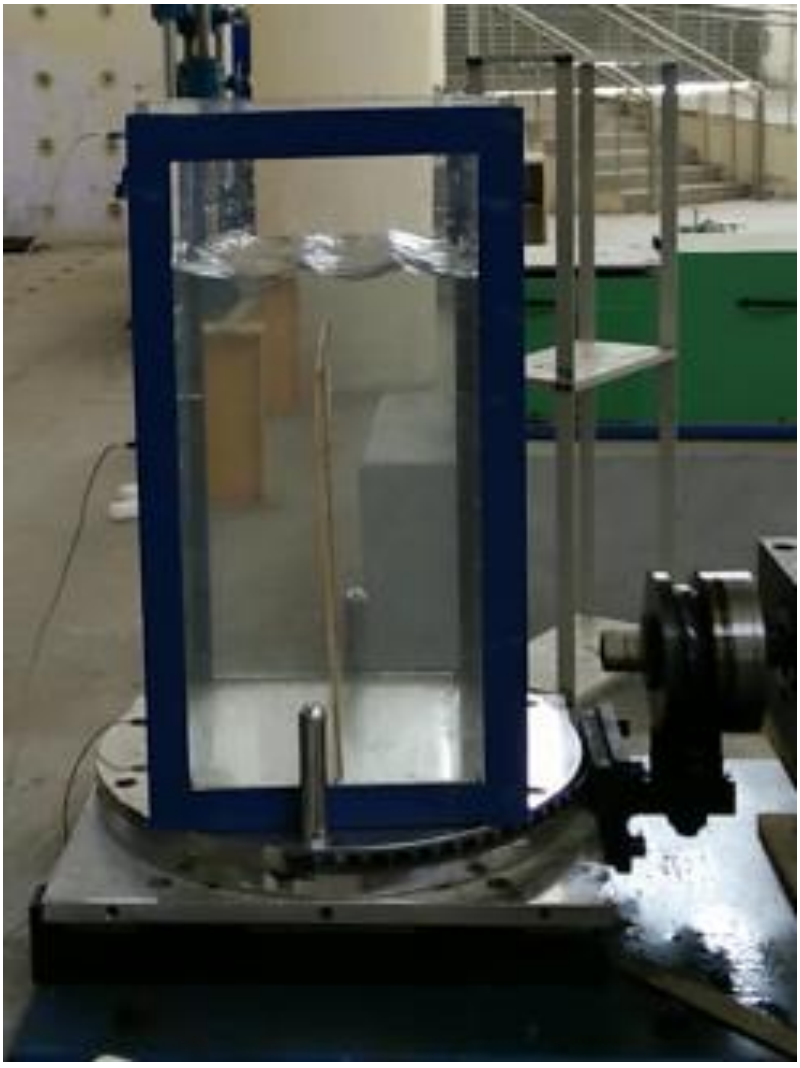

Figure 5.10: Surface profile at 80% fill at frequency 4.4Hz with baffle height 0.4m

Figure 5.11 shows the surface profile of the liquid free surface when the tank is provided with 0.4m high baffle and is seismically excited with 2.8Hz frequency. In this case the tank fill level is 50%.

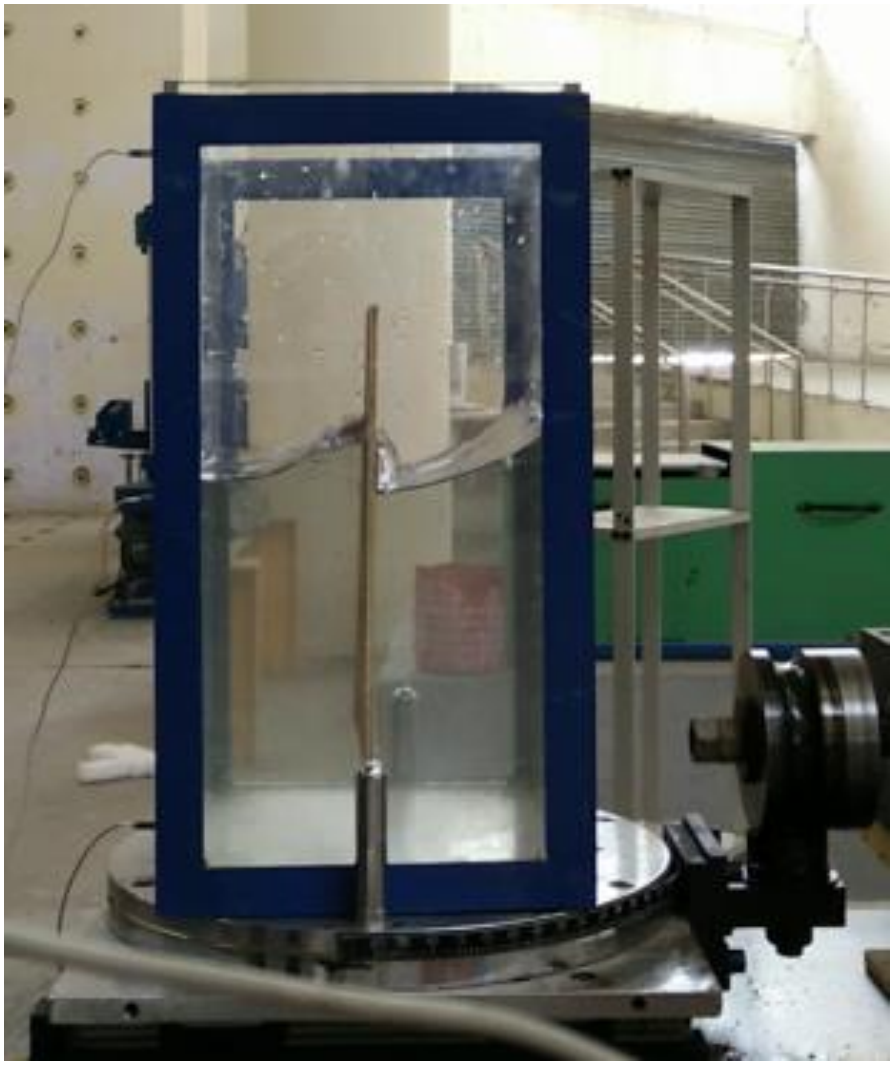

Figure 5.11: Surface profile at 50% fill at frequency 2.8Hz with baffle height 0.4m

Figure 5.12 shows the surface profile of the liquid free surface when the tank is provided with 0.4m high baffle and is seismically excited with 4.4Hz frequency. In this case the tank fill level is 50%.

Figure 5.12: Surface profile at 50% fill at frequency 4.4Hz with baffle height 0.4m

5.4 Readings obtained

The tank is provided with three accelerometers on the left wall the tank. These accelerometers are connected to the amplifier which is connected to the computer. The software used in this study is OROS NVGate. This software records the accelerations of the surface to which the accelerometers are attached. The values of accelerations obtained are in terms of factors of gravity (g) and their unit is m/s^2. The readings are in decimal values so we have converted them into the unit mm/s^2 so as to facilitate their analysis. Then these readings are plotted on graphs with respect to time. The graphs have been plotted in excel and are given in chapter 6. The first column of the following tables consist of the time of excitation which is at 0.5 second interval. The second, third and fourth columns consist of values of accelerations at 0.5 second interval corresponding to three accelerometers.

Table 5.2 to 5.13 provide the data obtained from the software for different cases. Each table is given with the variation in parameters. The parameters taken into account are percentage of fill of tank, excitation frequency, presence or absence of baffle and height of baffle if used.

Table 5.2: Variation of acceleration with time at 50% fill at *f*n= 2.8Hz

Time	Acceleration(1)	Acceleration(2)	Acceleration(3)
s	g mm/s^2	g mm/s^2	g mm/s^2
5.00E-01	-2.03E-01	-9.79E+00	-1.28E+00
1.00E+00	-1.71E-03	-1.29E-03	-1.79E-02
1.50E+00	1.41E-03	1.27E-03	1.59E-02
2.00E+00	1.96E-03	1.20E-03	1.47E-02
2.50E+00	-1.35E-02	-1.25E-03	-2.02E-02
3.00E+00	-1.65E-03	-1.08E-03	-1.19E-02
3.50E+00	-2.24E-02	-1.19E-03	-2.48E-02
4.00E+00	3.31E-02	1.31E-03	4.71E-02
4.50E+00	3.53E-02	1.31E-03	4.66E-02
5.00E+00	-3.60E-02	-1.42E-03	-4.00E-02
5.50E+00	-3.21E-02	-1.35E-03	-3.88E-02
6.00E+00	-5.21E-02	-1.20E-03	-5.99E-02
6.50E+00	4.23E-02	1.11E-03	7.00E-02
7.00E+00	4.33E-02	1.20E-03	6.25E-02
7.50E+00	6.46E-02	1.14E-03	6.73E-02
8.00E+00	-7.49E-02	-1.31E-03	-1.64E-01
8.50E+00	-7.65E-02	-4.00E+00	-2.22E-01
9.00E+00	1.32E-01	3.98E+00	3.44E-01
9.50E+00	1.51E-01	2.99E+00	4.14E-01
1.00E+01	1.36E-01	2.39E+00	4.79E-01
1.05E+01	-1.00E-01	-2.97E-01	-4.96E-01
1.10E+01	-1.06E-01	-1.89E-02	-4.07E-01
1.15E+01	-1.18E-01	-4.35E-03	-4.10E-01
1.20E+01	1.37E-01	1.34E+00	3.20E-01
1.25E+01	1.10E-01	1.05E+00	3.12E-01
1.30E+01	1.14E-01	1.62E+00	4.05E-01
1.35E+01	-1.09E-01	-5.32E-01	-4.33E-01
1.40E+01	-1.24E-01	-8.92E-01	-5.32E-01
1.45E+01	1.69E-01	1.18E+00	5.52E-01
1.50E+01	1.50E-01	2.07E+00	5.26E-01
1.55E+01	1.50E-01	1.99E+00	5.34E-01
1.60E+01	1.18E-01	6.60E-01	4.08E-01
1.65E+01	-1.32E-01	-8.32E-01	-4.36E-01
1.70E+01	-1.36E-01	-1.13E+00	-4.43E-01
1.75E+01	-1.33E-01	-8.47E-01	-6.57E-01
1.80E+01	1.47E-01	8.41E-01	7.65E-01
1.85E+01	1.79E-01	1.11E+00	1.03E+00
1.90E+01	1.89E-01	8.85E-01	1.07E+00
1.95E+01	-1.90E-01	-1.23E+00	-1.21E+00
2.00E+01	-1.79E-01	-1.12E+01	-1.33E+00

Table 5.3: Variation of acceleration with time at 80% fill at *f*n= 2.8Hz

Time	Acceleration(1)	Acceleration(2)	Acceleration(3)
s	g mm/s^2	g mm/s^2	g mm/s^2
5.00E-01	-2.32E-01	-1.07E+01	-1.66E+00
1.00E+00	-1.99E-01	-1.03E+00	-1.44E+00
1.50E+00	2.12E-01	7.74E-01	1.48E+00
2.00E+00	2.18E-01	7.71E-01	1.67E+00
2.50E+00	2.05E-01	7.95E-01	1.48E+00
3.00E+00	-2.67E-01	-9.21E-01	-1.72E+00
3.50E+00	-2.85E-01	-7.43E-01	-1.67E+00
4.00E+00	2.97E-01	9.46E-01	1.63E+00
4.50E+00	2.91E-01	7.55E+00	1.83E+00
5.00E+00	3.14E-01	8.00E-01	1.64E+00
5.50E+00	-3.61E-01	-1.42E+00	-1.87E+00
6.00E+00	-3.18E-01	-9.83E-01	-1.75E+00
6.50E+00	-3.13E-01	-9.08E-01	-1.83E+00
7.00E+00	2.72E-01	1.14E+00	1.95E+00
7.50E+00	2.38E-01	7.92E-01	1.78E+00
8.00E+00	3.33E-01	9.65E+00	2.09E+00
8.50E+00	-3.11E-01	-1.14E+01	-1.81E+00
9.00E+00	-2.88E-01	-9.58E+00	-2.09E+00
9.50E+00	3.03E-01	1.28E+01	1.85E+00
1.00E+01	3.29E-01	2.95E+01	2.03E+00
1.05E+01	3.50E-01	1.41E+01	1.94E+00
1.10E+01	-3.59E-01	-1.12E+01	-1.92E+00
1.15E+01	-3.01E-01	-9.96E+00	-1.99E+00
1.20E+01	3.09E-01	1.91E+01	1.83E+00
1.25E+01	3.30E-01	2.36E+01	2.05E+00
1.30E+01	-2.80E-01	-7.37E+00	-1.77E+00
1.35E+01	-3.36E-01	-1.45E+01	-2.07E+00
1.40E+01	3.27E-01	2.18E+01	1.79E+00
1.45E+01	2.30E-01	1.61E+01	2.04E+00
1.50E+01	2.76E-01	1.41E+01	1.79E+00
1.55E+01	-3.49E-01	-1.02E+01	-2.02E+00
1.60E+01	-2.30E-01	-2.74E+01	-1.85E+00
1.65E+01	-2.05E-01	-4.73E+00	-1.92E+00
1.70E+01	3.19E-01	3.01E+00	1.88E+00
1.75E+01	3.13E-01	1.18E+00	1.83E+00
1.80E+01	-2.83E-01	-9.86E-01	-1.91E+00
1.85E+01	-2.12E-01	-1.40E+00	-1.73E+00
1.90E+01	3.09E-01	1.09E+00	1.92E+00
1.95E+01	3.19E-01	1.53E+01	1.68E+00
2.00E+01	2.43E-01	1.24E+01	1.93E+00

Table 5.4: Variation of acceleration with time at 50% fill at f_n= 4.4Hz

Time	Acceleration(1)	Acceleration(2)	Acceleration(3)
s	g mm/s^2	g mm/s^2	g mm/s^2
5.00E-01	-2.43E-01	-1.42E+00	-9.18E-01
1.00E+00	-2.55E-01	-9.36E+00	-1.67E+00
1.50E+00	2.19E-01	8.63E-01	1.92E+00
2.00E+00	2.48E-01	4.07E+00	1.72E+00
2.50E+00	-3.05E-01	-1.07E+00	-1.86E+00
3.00E+00	-2.54E-01	-3.26E+00	-1.78E+00
3.50E+00	2.39E-01	7.78E-01	1.82E+00
4.00E+00	2.88E-01	1.97E+00	1.86E+00
4.50E+00	3.08E-01	8.55E-01	1.77E+00
5.00E+00	-2.50E-01	-9.29E-01	-1.93E+00
5.50E+00	-2.27E-01	-2.11E+00	-1.73E+00
6.00E+00	-3.24E-01	-2.76E+00	-1.98E+00
6.50E+00	3.06E-01	1.76E+00	1.70E+00
7.00E+00	2.50E-01	2.92E+00	1.98E+00
7.50E+00	-2.44E-01	-1.40E+00	-1.71E+00
8.00E+00	-3.16E-01	-1.04E+00	-1.97E+00
8.50E+00	2.90E-01	1.15E+01	1.76E+00
9.00E+00	2.23E-01	1.00E+00	1.94E+00
9.50E+00	2.65E-01	6.76E+00	1.83E+00
1.00E+01	-3.11E-01	-2.28E+00	-1.87E+00
1.05E+01	-2.54E-01	-8.67E-01	-1.90E+00
1.10E+01	2.17E-01	1.24E+01	1.82E+00
1.15E+01	3.04E-01	4.33E+00	1.96E+00
1.20E+01	-3.17E-01	-3.00E+01	-1.77E+00
1.25E+01	-2.56E-01	-1.51E+01	-1.99E+00
1.30E+01	-2.17E-01	-5.05E+00	-1.70E+00
1.35E+01	3.26E-01	1.22E+00	1.99E+00
1.40E+01	2.89E-01	8.07E-01	1.71E+00
1.45E+01	-2.40E-01	-8.62E+00	-1.98E+00
1.50E+01	-2.55E-01	-1.02E+01	-1.73E+00
1.55E+01	3.18E-01	1.68E+00	1.95E+00
1.60E+01	2.56E-01	1.80E+01	1.78E+00
1.65E+01	2.02E-01	6.88E+00	1.89E+00
1.70E+01	-2.82E-01	-4.42E+00	-1.76E+00
1.75E+01	-2.68E-01	-5.82E-01	-1.50E+00
1.80E+01	-2.76E-01	-8.39E-01	-1.51E+00
1.85E+01	2.22E-01	6.42E-01	1.19E+00
1.90E+01	2.24E-01	6.79E-01	1.21E+00
1.95E+01	-2.40E-01	-7.94E-01	-1.01E+00
2.00E+01	-2.70E-01	-7.16E-01	-9.89E-01

Table 5.5: Variation of acceleration with time at 80% fill at *f*n= 4.4Hz

Time	Acceleration(1)	Acceleration(2)	Acceleration(3)
s	g mm/s^2	g mm/s^2	g mm/s^2
5.00E-01	-4.13E-01	-1.04E+00	-7.99E-01
1.00E+00	-2.66E-01	-1.17E+00	-8.35E-01
1.50E+00	-3.11E-01	-1.94E+00	-6.79E-01
2.00E+00	2.84E-01	3.18E+00	7.69E-01
2.50E+00	2.97E-01	1.14E+00	7.12E-01
3.00E+00	-3.82E-01	-8.02E-01	-6.72E-01
3.50E+00	-3.99E-01	-8.20E-01	-7.09E-01
4.00E+00	3.84E-01	6.98E-01	6.52E-01
4.50E+00	4.54E-01	6.92E-01	7.12E-01
5.00E+00	4.03E-01	7.77E-01	7.18E-01
5.50E+00	-4.34E-01	-7.91E-01	-7.26E-01
6.00E+00	-4.23E-01	-7.44E-01	-6.94E-01
6.50E+00	-4.12E-01	-7.14E-01	-6.95E-01
7.00E+00	4.03E-01	6.99E-01	6.58E-01
7.50E+00	4.16E-01	8.07E-01	5.82E-01
8.00E+00	-4.34E-01	-7.76E-01	-6.88E-01
8.50E+00	-4.44E-01	-8.23E-01	-6.94E-01
9.00E+00	4.12E-01	6.81E-01	5.22E-01
9.50E+00	4.22E-01	7.62E-01	6.54E-01
1.00E+01	4.22E-01	7.53E-01	6.51E-01
1.05E+01	-3.99E-01	-7.52E-01	-5.44E-01
1.10E+01	-4.31E-01	-6.66E-01	-5.77E-01
1.15E+01	4.03E-01	6.69E-01	5.83E-01
1.20E+01	4.16E-01	7.21E-01	5.62E-01
1.25E+01	-4.15E-01	-6.93E-01	-5.56E-01
1.30E+01	-4.43E-01	-6.87E-01	-5.04E-01
1.35E+01	-4.08E-01	-7.78E-01	-5.47E-01
1.40E+01	4.03E-01	6.78E-01	6.23E-01
1.45E+01	4.41E-01	7.95E-01	8.66E-01
1.50E+01	-4.51E-01	-7.93E-01	-1.03E+00
1.55E+01	-4.33E-01	-7.57E-01	-1.04E+00
1.60E+01	4.30E-01	7.43E-01	9.14E-01
1.65E+01	4.31E-01	7.77E-01	7.40E-01
1.70E+01	4.24E-01	8.61E-01	6.69E-01
1.75E+01	-4.18E-01	-8.35E-01	-6.74E-01
1.80E+01	-4.42E-01	-6.89E-01	-7.80E-01
1.85E+01	-4.13E-01	-7.02E-01	-8.20E-01
1.90E+01	4.42E-01	8.21E-01	8.60E-01
1.95E+01	4.47E-01	8.60E-01	8.86E-01
2.00E+01	-4.22E-01	-8.92E-01	-8.18E-01

Table 5.6: Variation of acceleration with time at 50% fill with 0.3m baffle at *f*n= 2.8Hz

Time	Acceleration(1)	Acceleration(2)	Acceleration(3)
s	g mm/s^2	g mm/s^2	g mm/s^2
5.00E-01	-5.05E-01	-3.92E+00	-2.41E+00
1.00E+00	-4.28E-01	-8.56E-01	-8.11E-01
1.50E+00	4.30E-01	8.76E-01	7.10E-01
2.00E+00	4.18E-01	8.22E-01	6.11E-01
2.50E+00	4.17E-01	8.12E-01	6.46E-01
3.00E+00	-4.33E-01	-8.56E-01	-7.52E-01
3.50E+00	-4.27E-01	-6.80E-01	-7.92E-01
4.00E+00	-4.14E-01	-6.21E-01	-8.23E-01
4.50E+00	3.99E-01	5.88E-01	8.04E-01
5.00E+00	4.13E-01	6.60E-01	7.42E-01
5.50E+00	-3.84E-01	-6.67E-01	-7.25E-01
6.00E+00	-4.52E-01	-7.18E-01	-1.02E+00
6.50E+00	4.68E-01	8.45E-01	1.10E+00
7.00E+00	4.98E-01	8.53E-01	9.57E-01
7.50E+00	5.19E-01	6.44E-01	9.86E-01
8.00E+00	-5.02E-01	-6.71E-01	-6.69E-01
8.50E+00	-5.75E-01	-7.93E-01	-8.06E-01
9.00E+00	5.15E-01	6.74E-01	7.14E-01
9.50E+00	4.83E-01	7.26E-01	4.80E-01
1.00E+01	5.44E-01	7.34E-01	4.91E-01
1.05E+01	-5.74E-01	-7.41E-01	-7.24E-01
1.10E+01	-4.99E-01	-8.43E-01	-1.33E+00
1.15E+01	-5.05E-01	-7.97E-01	-1.89E+00
1.20E+01	4.97E-01	6.63E+00	1.15E+00
1.25E+01	5.36E-01	3.63E+00	1.39E+00
1.30E+01	-4.74E-01	-1.46E+00	-1.52E+00
1.35E+01	-4.85E-01	-1.43E+00	-1.62E+00
1.40E+01	5.06E-01	1.61E+00	2.08E+00
1.45E+01	5.14E-01	1.46E+00	1.87E+00
1.50E+01	5.07E-01	1.37E+00	1.64E+00
1.55E+01	-4.62E-01	-5.27E+00	-2.02E+00
1.60E+01	-4.94E-01	-1.66E+01	-2.04E+00
1.65E+01	5.04E-01	1.61E+00	1.71E+00
1.70E+01	5.13E-01	7.37E-01	1.67E+00
1.75E+01	-4.97E-01	-6.75E-01	-2.05E+00
1.80E+01	-5.08E-01	-6.16E-01	-2.13E+00
1.85E+01	-5.05E-01	-7.11E-01	-1.98E+00
1.90E+01	5.24E-01	7.87E-01	2.05E+00
1.95E+01	5.08E-01	7.68E-01	2.16E+00
2.00E+01	5.11E-01	1.19E+01	2.23E+00

Table 5.7: Variation of acceleration with time at 80% fill with 0.3m baffle at *f*n= 2.8Hz

Time	Acceleration(1)	Acceleration(2)	Acceleration(3)
s	g mm/s^2	g mm/s^2	g mm/s^2
5.00E-01	-4.77E-03	-2.07E-01	-1.51E-01
1.00E+00	-5.08E-01	-1.45E+00	-2.05E+00
1.50E+00	4.93E-01	1.32E+00	1.85E+00
2.00E+00	4.75E-01	1.30E+00	1.83E+00
2.50E+00	-5.36E-01	-8.23E-01	-1.21E+00
3.00E+00	-5.31E-01	-8.24E-01	-1.23E+00
3.50E+00	-5.29E-01	-7.98E-01	-1.01E+00
4.00E+00	5.40E-01	8.33E-01	1.15E+00
4.50E+00	5.34E-01	7.80E-01	1.07E+00
5.00E+00	-5.11E-01	-8.01E-01	-1.11E+00
5.50E+00	-5.06E-01	-1.14E+00	-1.63E+00
6.00E+00	5.10E-01	1.08E+00	1.62E+00
6.50E+00	5.06E-01	8.65E-01	1.29E+00
7.00E+00	-5.21E-01	-1.10E+00	-1.61E+00
7.50E+00	-5.17E-01	-1.20E+00	-1.79E+00
8.00E+00	-4.97E-01	-9.33E-01	-1.41E+00
8.50E+00	4.94E-01	9.46E-01	1.42E+00
9.00E+00	5.02E-01	9.70E-01	1.51E+00
9.50E+00	-5.35E-01	-9.62E-01	-1.46E+00
1.00E+01	-5.24E-01	-1.11E+00	-1.70E+00
1.05E+01	5.40E-01	1.04E+00	1.63E+00
1.10E+01	5.24E-01	9.95E-01	1.57E+00
1.15E+01	5.24E-01	1.00E+00	1.57E+00
1.20E+01	-5.31E-01	-1.08E+00	-1.69E+00
1.25E+01	-5.46E-01	-9.47E-01	-1.55E+00
1.30E+01	5.38E-01	8.18E-01	1.36E+00
1.35E+01	5.25E-01	8.71E-01	1.44E+00
1.40E+01	-5.40E-01	-8.58E-01	-1.39E+00
1.45E+01	-5.41E-01	-8.98E-01	-1.45E+00
1.50E+01	5.27E-01	6.86E-01	1.10E+00
1.55E+01	3.16E-01	9.73E-01	8.00E-01
1.60E+01	1.18E-01	9.32E-01	7.03E-01
1.65E+01	-4.07E-02	-7.32E-01	-5.32E-01
1.70E+01	-3.01E-02	-5.48E-01	-5.00E-01
1.75E+01	1.63E-02	5.10E-01	3.97E-01
1.80E+01	1.42E-02	4.22E-01	3.40E-01
1.85E+01	-9.89E-03	-3.36E-01	-3.00E-01
1.90E+01	-8.98E-03	-3.17E-01	-2.38E-01
1.95E+01	-6.95E-03	-2.55E-01	-2.17E-01
2.00E+01	6.05E-03	2.20E-01	1.85E-01

Table 5.8: Variation of acceleration with time at 50% fill with 0.3m baffle at *f*n=4.4Hz

Time	Acceleration(1)	Acceleration(2)	Acceleration(3)
s	g mm/s^2	g mm/s^2	g mm/s^2
5.00E-01	-1.31E-03	-2.63E-01	-2.09E-02
1.00E+00	-3.89E-03	-1.61E-01	-1.21E-01
1.50E+00	-3.29E-03	-1.47E-01	-1.17E-01
2.00E+00	3.34E-03	1.26E-01	1.08E-01
2.50E+00	2.64E-03	1.25E-01	9.56E-02
3.00E+00	-2.52E-03	-1.08E-01	-9.23E-02
3.50E+00	-2.05E-03	-9.42E-02	-7.94E-02
4.00E+00	1.95E-03	8.82E-02	7.19E-02
4.50E+00	1.71E-03	7.18E-02	6.77E-02
5.00E+00	1.57E-03	6.78E-02	5.80E-02
5.50E+00	-1.98E-03	-6.33E-02	-5.98E-02
6.00E+00	-1.49E-03	-5.62E-02	-5.51E-02
6.50E+00	1.73E-03	5.78E-02	5.43E-02
7.00E+00	1.44E-03	5.33E-02	5.53E-02
7.50E+00	-1.40E-03	-4.80E-02	-4.86E-02
8.00E+00	-1.55E-03	-4.62E-02	-4.97E-02
8.50E+00	-1.61E-03	-3.89E-02	-4.55E-02
9.00E+00	1.46E-03	3.42E-02	4.08E-02
9.50E+00	1.64E-03	3.24E-02	4.29E-02
1.00E+01	-3.16E-03	-2.79E-02	-3.87E-02
1.05E+01	-3.61E-03	-2.96E-02	-4.08E-02
1.10E+01	3.67E-03	2.88E-02	4.07E-02
1.15E+01	4.28E-03	2.74E-02	3.78E-02
1.20E+01	1.02E-02	2.83E-02	3.83E-02
1.25E+01	-2.46E-02	-1.76E+01	-3.36E-02
1.30E+01	-1.13E-02	-2.02E+01	-3.53E-02
1.35E+01	6.54E-03	2.16E+00	3.21E-02
1.40E+01	6.27E-03	1.07E+00	3.03E-02
1.45E+01	-4.88E-03	-8.98E-01	-3.17E-02
1.50E+01	-1.50E-03	-1.00E+00	-3.09E-02
1.55E+01	-3.16E-03	-6.87E-01	-2.82E-02
1.60E+01	2.35E-03	5.54E-01	3.04E-02
1.65E+01	1.70E-03	6.01E-01	2.68E-02
1.70E+01	-1.36E-03	-6.73E-01	-2.64E-02
1.75E+01	-1.05E-03	-8.82E-01	-2.70E-02
1.80E+01	1.14E-03	9.42E-02	2.35E-02
1.85E+01	1.26E-03	4.59E-01	2.54E-02
1.90E+01	9.76E-04	3.87E-01	2.37E-02
1.95E+01	-1.27E-03	-1.73E-01	-2.22E-02
2.00E+01	-1.33E-03	-2.98E-01	-2.42E-02

Table 5.9: Variation of acceleration with time at 80% fill with 0.3m baffle at *f*n=4.4Hz

Time	Acceleration(1)	Acceleration(2)	Acceleration(3)
s	g mm/s^2	g mm/s^2	g mm/s^2
5.00E-01	-1.05E-03	-3.14E-01	-6.46E-03
1.00E+00	1.37E-03	3.00E-01	2.20E-02
1.50E+00	1.32E-03	1.84E-01	1.92E-02
2.00E+00	1.70E-03	2.81E-01	2.05E-02
2.50E+00	-1.41E-03	-1.88E-01	-1.92E-02
3.00E+00	-1.39E-03	-2.65E-01	-1.78E-02
3.50E+00	1.63E-03	3.92E-01	1.95E-02
4.00E+00	1.52E-03	2.44E-01	1.70E-02
4.50E+00	-1.48E-03	-3.30E-01	-1.74E-02
5.00E+00	-1.57E-03	-1.49E-01	-1.75E-02
5.50E+00	-1.25E-03	-1.61E-01	-1.54E-02
6.00E+00	1.41E-03	1.27E-01	1.66E-02
6.50E+00	2.43E-03	4.19E-01	1.46E-02
7.00E+00	-2.87E-03	-1.22E+00	-1.58E-02
7.50E+00	-1.79E-03	-3.46E-01	-1.54E-02
8.00E+00	1.07E-03	2.04E-01	1.38E-02
8.50E+00	9.78E-04	1.70E-01	1.42E-02
9.00E+00	1.33E-03	1.45E-01	1.44E-02
9.50E+00	-9.41E-04	-1.69E-01	-1.26E-02
1.00E+01	-1.18E-03	-1.54E-01	-1.36E-02
1.05E+01	1.03E-03	1.73E-01	1.29E-02
1.10E+01	1.17E-03	2.04E-01	1.18E-02
1.15E+01	-1.05E-03	-2.45E-01	-1.26E-02
1.20E+01	-1.13E-03	-2.24E-01	-1.10E-02
1.25E+01	-8.15E-04	-2.83E-01	-1.10E-02
1.30E+01	1.01E-03	2.28E-01	1.19E-02
1.35E+01	9.68E-04	2.48E-01	1.04E-02
1.40E+01	-1.09E-03	-1.82E-01	-1.05E-02
1.45E+01	-1.00E-03	-1.72E-01	-1.05E-02
1.50E+01	8.15E-04	1.67E-01	9.28E-03
1.55E+01	1.16E-03	2.24E-01	1.02E-02
1.60E+01	9.83E-04	2.28E-01	9.18E-03
1.65E+01	-1.08E-03	-2.55E-01	-8.84E-03
1.70E+01	-8.93E-04	-1.79E-01	-9.30E-03
1.75E+01	1.02E-03	1.75E-01	8.00E-03
1.80E+01	8.21E-04	1.34E-01	8.52E-03
1.85E+01	-1.04E-03	-1.60E-01	-8.06E-03
1.90E+01	-1.07E-03	-2.18E-01	-7.41E-03
1.95E+01	8.75E-04	2.09E-01	7.89E-03
2.00E+01	1.03E-03	1.83E-01	7.29E-03

Table 5.10: Variation of acceleration with time at 50% fill with 0.4m baffle at *f*n=2.8Hz

Time	Acceleration(1)	Acceleration(2)	Acceleration(3)
s	g mm/s^2	g mm/s^2	g mm/s^2
5.00E-01	5.19E-01	6.44E-01	9.86E-01
1.00E+00	-4.94E-01	-9.46E-01	-1.42E+00
1.50E+00	-5.02E-01	-9.70E-01	-1.51E+00
2.00E+00	5.35E-01	9.62E-01	1.46E+00
2.50E+00	5.24E-01	1.11E+00	1.70E+00
3.00E+00	5.40E-01	1.04E+00	1.63E+00
3.50E+00	-5.24E-01	-9.95E-01	-1.57E+00
4.00E+00	-5.24E-01	-1.00E+00	-1.57E+00
4.50E+00	5.31E-01	1.08E+00	1.69E+00
5.00E+00	5.46E-01	9.47E-01	1.55E+00
5.50E+00	-5.38E-01	-8.18E-01	-1.36E+00
6.00E+00	-5.25E-01	-8.71E-01	-1.44E+00
6.50E+00	-5.40E-01	-8.58E-01	-1.39E+00
7.00E+00	5.41E-01	8.98E-01	1.45E+00
7.50E+00	5.27E-01	6.86E-01	1.10E+00
8.00E+00	-3.16E-01	-9.73E-01	-8.00E-01
8.50E+00	-1.18E-01	-9.32E-01	-7.03E-01
9.00E+00	4.07E-02	7.32E-01	5.32E-01
9.50E+00	3.01E-02	5.48E-01	5.00E-01
1.00E+01	1.63E-02	5.10E-01	3.97E-01
1.05E+01	-1.42E-02	-4.22E-01	-3.40E-01
1.10E+01	-9.89E-03	-3.36E-01	-3.00E-01
1.15E+01	8.98E-03	3.17E-01	2.38E-01
1.20E+01	6.95E-03	2.55E-01	2.17E-01
1.25E+01	-6.05E-03	-2.20E-01	-1.85E-01
1.30E+01	-4.77E-03	-2.07E-01	-1.51E-01
1.35E+01	-4.68E-03	-1.64E-01	-1.46E-01
1.40E+01	4.28E-01	8.56E-01	8.11E-01
1.45E+01	4.30E-01	8.76E-01	7.10E-01
1.50E+01	-4.18E-01	-8.22E-01	-6.11E-01
1.55E+01	-4.17E-01	-8.12E-01	-6.46E-01
1.60E+01	4.33E-01	8.56E-01	7.52E-01
1.65E+01	4.27E-01	6.80E-01	7.92E-01
1.70E+01	4.14E-01	6.21E-01	8.23E-01
1.75E+01	-3.99E-01	-5.88E-01	-8.04E-01
1.80E+01	-4.13E-01	-6.60E-01	-7.42E-01
1.85E+01	3.84E-01	6.67E-01	7.25E-01
1.90E+01	4.52E-01	7.18E-01	1.02E+00
1.95E+01	4.68E-01	8.45E-01	1.10E+00
2.00E+01	-4.98E-01	-8.53E-01	-9.57E-01

Table 5.11: Variation of acceleration with time at 80% fill with 0.4m baffle at *f*n= 2.8Hz

Time	Acceleration(1)	Acceleration(2)	Acceleration(3)
s	g mm/s^2	g mm/s^2	g mm/s^2
5.00E-01	-1.46E-03	-3.42E-02	-4.08E-02
1.00E+00	-5.75E-01	-7.93E-01	-8.06E-01
1.50E+00	5.15E-01	6.74E-01	7.14E-01
2.00E+00	4.83E-01	7.26E-01	4.80E-01
2.50E+00	-5.44E-01	-7.34E-01	-4.91E-01
3.00E+00	-5.74E-01	-7.41E-01	-7.24E-01
3.50E+00	-4.99E-01	-8.43E-01	-1.33E+00
4.00E+00	5.05E-01	7.97E-01	1.89E+00
4.50E+00	4.97E-01	6.63E+00	1.15E+00
5.00E+00	-1.37E-03	-3.00E-01	-2.20E-02
5.50E+00	-1.32E-03	-1.84E-01	-1.92E-02
6.00E+00	1.70E-03	2.81E-01	2.05E-02
6.50E+00	1.41E-03	1.88E-01	1.92E-02
7.00E+00	1.39E-03	2.65E-01	1.78E-02
7.50E+00	-1.63E-03	-3.92E-01	-1.95E-02
8.00E+00	-1.52E-03	-2.44E-01	-1.70E-02
8.50E+00	1.48E-03	3.30E-01	1.74E-02
9.00E+00	1.57E-03	1.49E-01	1.75E-02
9.50E+00	-1.25E-03	-1.61E-01	-1.54E-02
1.00E+01	-1.41E-03	-1.27E-01	-1.66E-02
1.05E+01	2.43E-03	4.19E-01	1.46E-02
1.10E+01	2.87E-03	1.22E+00	1.58E-02
1.15E+01	1.79E-03	3.46E-01	1.54E-02
1.20E+01	-1.07E-03	-2.04E-01	-1.38E-02
1.25E+01	-9.78E-04	-1.70E-01	-1.42E-02
1.30E+01	1.33E-03	1.45E-01	1.44E-02
1.35E+01	9.41E-04	1.69E-01	1.26E-02
1.40E+01	-1.18E-03	-1.54E-01	-1.36E-02
1.45E+01	-1.03E-03	-1.73E-01	-1.29E-02
1.50E+01	-1.17E-03	-2.04E-01	-1.18E-02
1.55E+01	1.05E-03	2.45E-01	1.26E-02
1.60E+01	1.13E-03	2.24E-01	1.10E-02
1.65E+01	-8.15E-04	-2.83E-01	-1.10E-02
1.70E+01	-1.01E-03	-2.28E-01	-1.19E-02
1.75E+01	9.68E-04	2.48E-01	1.04E-02
1.80E+01	1.73E-03	5.78E-02	5.43E-02
1.85E+01	1.44E-03	5.33E-02	5.53E-02
1.90E+01	-1.40E-03	-4.80E-02	-4.86E-02
1.95E+01	-1.55E-03	-4.62E-02	-4.97E-02
2.00E+01	-1.61E-03	-3.89E-02	-4.55E-02

Table 5.12: Variation of acceleration with time at 50% fill with 0.4m baffle at *f*n= 4.4Hz

Time	Acceleration(1)	Acceleration(2)	Acceleration(3)
s	g mm/s^2	g mm/s^2	g mm/s^2
5.00E-01	1.18E-03	1.54E-01	1.36E-02
1.00E+00	3.16E-03	2.79E-02	3.87E-02
1.50E+00	-3.61E-03	-2.96E-02	-4.08E-02
2.00E+00	-3.67E-03	-2.88E-02	-4.07E-02
2.50E+00	-4.28E-03	-2.74E-02	-3.78E-02
3.00E+00	1.02E-02	2.83E-02	3.83E-02
3.50E+00	2.46E-02	1.76E+01	3.36E-02
4.00E+00	-4.28E-01	-8.56E-01	-8.11E-01
4.50E+00	-4.30E-01	-8.76E-01	-7.10E-01
5.00E+00	4.18E-01	8.22E-01	6.11E-01
5.50E+00	4.17E-01	8.12E-01	6.46E-01
6.00E+00	4.33E-01	8.56E-01	7.52E-01
6.50E+00	-4.27E-01	-6.80E-01	-7.92E-01
7.00E+00	-4.14E-01	-6.21E-01	-8.23E-01
7.50E+00	3.99E-01	5.88E-01	8.04E-01
8.00E+00	4.13E-01	6.60E-01	7.42E-01
8.50E+00	-3.84E-01	-6.67E-01	-7.25E-01
9.00E+00	-4.52E-01	-7.18E-01	-1.02E+00
9.50E+00	-4.68E-01	-8.45E-01	-1.10E+00
1.00E+01	4.98E-01	8.53E-01	9.57E-01
1.05E+01	5.19E-01	6.44E-01	9.86E-01
1.10E+01	-5.02E-01	-6.71E-01	-6.69E-01
1.15E+01	-5.75E-01	-7.93E-01	-8.06E-01
1.20E+01	5.15E-01	6.74E-01	7.14E-01
1.25E+01	4.83E-01	7.26E-01	4.80E-01
1.30E+01	5.44E-01	7.34E-01	4.91E-01
1.35E+01	-5.74E-01	-7.41E-01	-7.24E-01
1.40E+01	-4.99E-01	-8.43E-01	-1.33E+00
1.45E+01	5.05E-01	7.97E-01	1.89E+00
1.50E+01	4.97E-01	6.63E+00	1.15E+00
1.55E+01	5.36E-01	3.63E+00	1.39E+00
1.60E+01	-4.74E-01	-1.46E+00	-1.52E+00
1.65E+01	-4.85E-01	-1.43E+00	-1.62E+00
1.70E+01	5.06E-01	1.61E+00	2.08E+00
1.75E+01	5.14E-01	1.46E+00	1.87E+00
1.80E+01	-5.07E-01	-1.37E+00	-1.64E+00
1.85E+01	-4.62E-01	-5.27E+00	-2.02E+00
1.90E+01	-4.94E-01	-1.66E+01	-2.04E+00
1.95E+01	5.04E-01	1.61E+00	1.71E+00
2.00E+01	5.13E-01	7.37E-01	1.67E+00

Table 5.13: Variation of acceleration with time at 80% fill with 0.4m baffle at *f*n= 4.4Hz

Time	Acceleration(1)	Acceleration(2)	Acceleration(3)
s	g mm/s^2	g mm/s^2	g mm/s^2
5.00E-01	-9.78E-04	-1.70E-01	-1.42E-02
1.00E+00	-1.17E-03	-2.04E-01	-1.18E-02
1.50E+00	1.05E-03	2.45E-01	1.26E-02
2.00E+00	1.13E-03	2.24E-01	1.10E-02
2.50E+00	-8.15E-04	-2.83E-01	-1.10E-02
3.00E+00	-1.01E-03	-2.28E-01	-1.19E-02
3.50E+00	-9.68E-04	-2.48E-01	-1.04E-02
4.00E+00	1.09E-03	1.82E-01	1.05E-02
4.50E+00	1.00E-03	1.72E-01	1.05E-02
5.00E+00	-8.15E-04	-1.67E-01	-9.28E-03
5.50E+00	-1.16E-03	-2.24E-01	-1.02E-02
6.00E+00	9.83E-04	2.28E-01	9.18E-03
6.50E+00	1.08E-03	2.55E-01	8.84E-03
7.00E+00	8.93E-04	1.79E-01	9.30E-03
7.50E+00	-1.02E-03	-1.75E-01	-8.00E-03
8.00E+00	-8.21E-04	-1.34E-01	-8.52E-03
8.50E+00	1.04E-03	1.60E-01	8.06E-03
9.00E+00	1.07E-03	2.18E-01	7.41E-03
9.50E+00	8.75E-04	2.09E-01	7.89E-03
1.00E+01	-1.03E-03	-1.83E-01	-7.29E-03
1.05E+01	-1.05E-03	-3.14E-01	-6.46E-03
1.10E+01	1.41E-03	2.08E-01	7.80E-03
1.15E+01	5.08E-01	1.45E+00	2.05E+00
1.20E+01	-4.93E-01	-1.32E+00	-1.85E+00
1.25E+01	-4.75E-01	-1.30E+00	-1.83E+00
1.30E+01	-5.36E-01	-8.23E-01	-1.21E+00
1.35E+01	5.31E-01	8.24E-01	1.23E+00
1.40E+01	5.29E-01	7.98E-01	1.01E+00
1.45E+01	-5.40E-01	-8.33E-01	-1.15E+00
1.50E+01	-5.34E-01	-7.80E-01	-1.07E+00
1.55E+01	5.11E-01	8.01E-01	1.11E+00
1.60E+01	5.06E-01	1.14E+00	1.63E+00
1.65E+01	5.10E-01	1.08E+00	1.62E+00
1.70E+01	-5.06E-01	-8.65E-01	-1.29E+00
1.75E+01	-5.21E-01	-1.10E+00	-1.61E+00
1.80E+01	5.17E-01	1.20E+00	1.79E+00
1.85E+01	4.97E-01	9.33E-01	1.41E+00
1.90E+01	-4.94E-01	-9.46E-01	-1.42E+00
1.95E+01	-5.02E-01	-9.70E-01	-1.51E+00
2.00E+01	-5.35E-01	-9.62E-01	-1.46E+00

CHAPTER 6

RESULTS AND DISCUSSION

The readings obtained from the OROS NVGate software are the values of accelerations in terms of gravity(g). These values are plotted against the time of excitation. Then comparison is done between different cases taken into account.

Table 6.1: Natural frequencies of liquid contained in rectangular tank:

Mode Number	Theoretical (Hz)	Experimental (Hz)
1	1.56	1.6
2	2.78	2.8
3	3.61	3.7
4	4.27	4.4

6.1 CASE 1: When the tank is subjected to seismic excitation of frequency 2.8Hz without baffle

6.1.1. Below fig 6.1 and fig 6.3 shows the graph for accelerations variation vs. time at different fill level 50% and 80%, when the tank is excited by natural frequency without baffle. Fig 6.2 and fig 6.4 shows the graph for the local maxima of acceleration obtained from fig 6.1 and fig 6.3. It also provides the trend line and their equation for the respective cases.

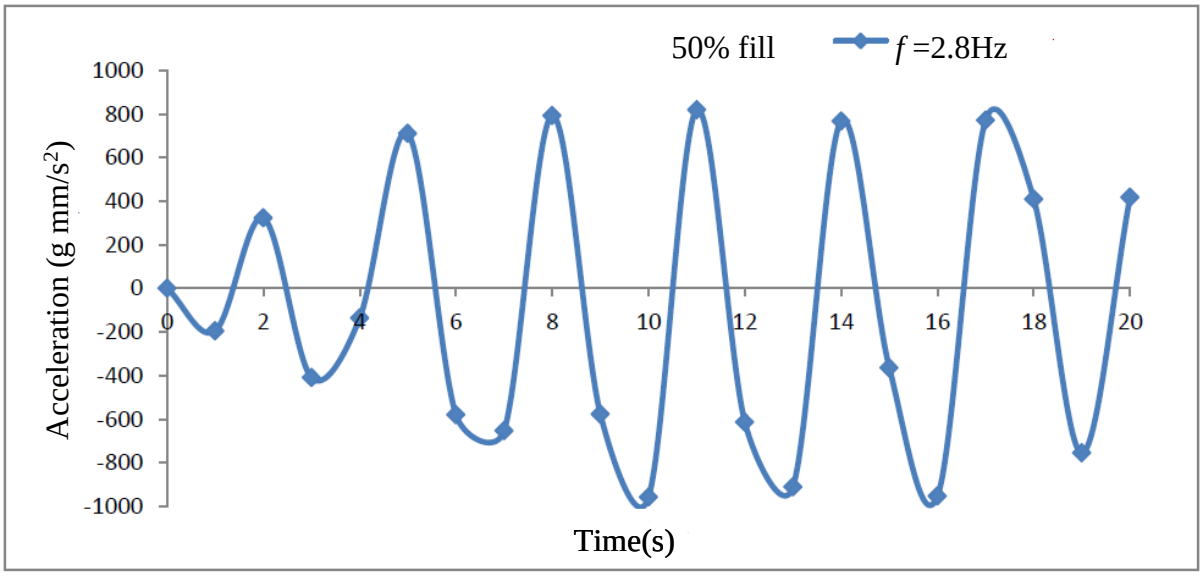

Figure 6.1: Accelerations at 50% fill at frequency 2.8Hz

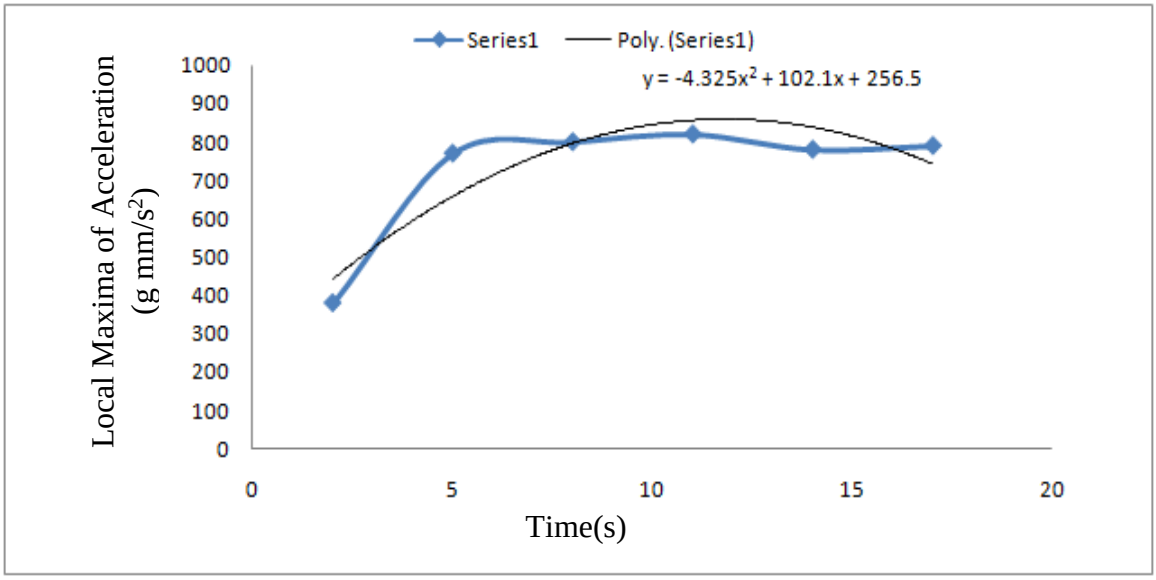

Figure 6.2: Trend line for local maxima of acceleration at 50% fill at frequency 2.8Hz

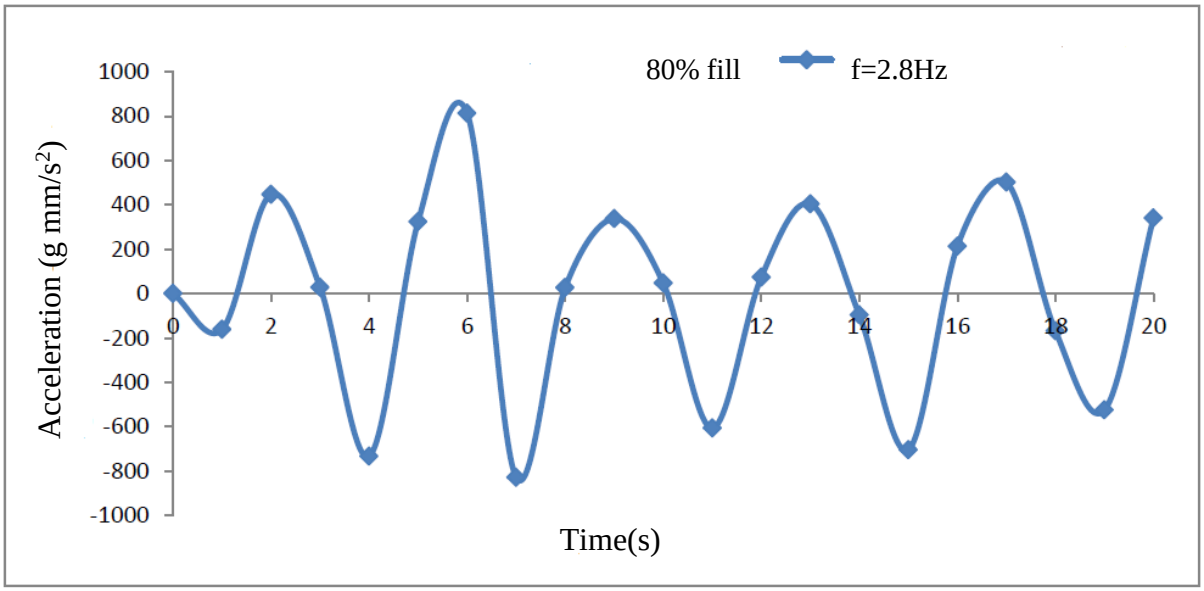

Figure 6.3: Accelerations at 80% fill at frequency 2.8Hz

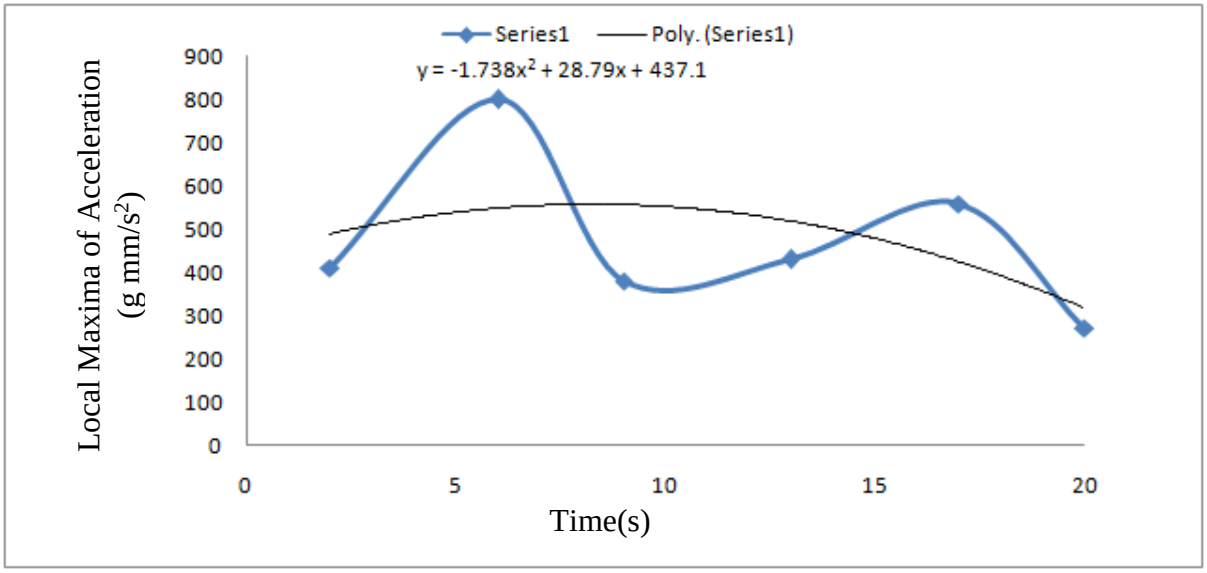

Figure 6.4: Trend line for local maxima of acceleration at 80% fill at frequency 2.8Hz

6.1.2 Fig 6.5 shows the comparison of accelerations for 50% fill and 80% fill condition, when the tank is seismically excited by frequency of 2.8Hz.

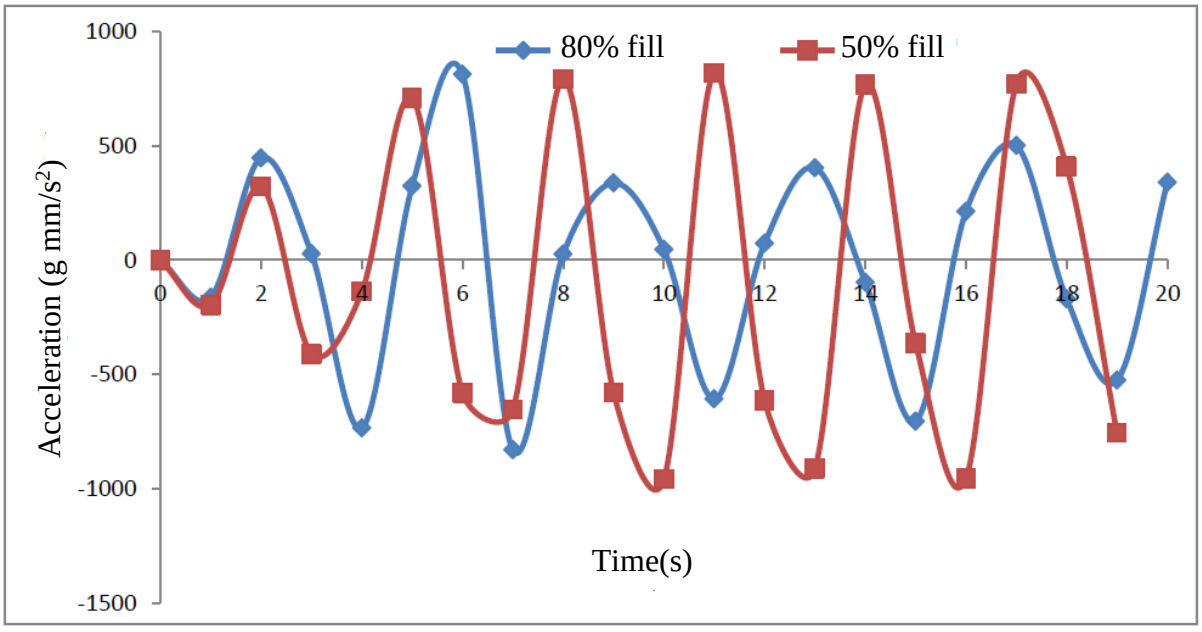

Figure 6.5: Accelerations at 50% and 80% fill at frequency 2.8Hz

From above graphs it is observed that maximum amplitude of acceleration is lower at higher fill level, because at higher fill level of fluid, slosh does not occur heavily.

6.2 CASE 2: When the tank is subjected to seismic excitation of frequency 4.4Hz without baffle

6.2.1. Below fig 6.6 and fig 6.8 shows the graph for accelerations variation vs. time at different fill level 50% and 80%, when the tank is excited by natural frequency without baffle. Fig 6.7 and fig 6.9 shows the graph for the local maxima of acceleration obtained from fig 6.6 and fig 6.8. It also provides the trend line and their equation for the respective cases.

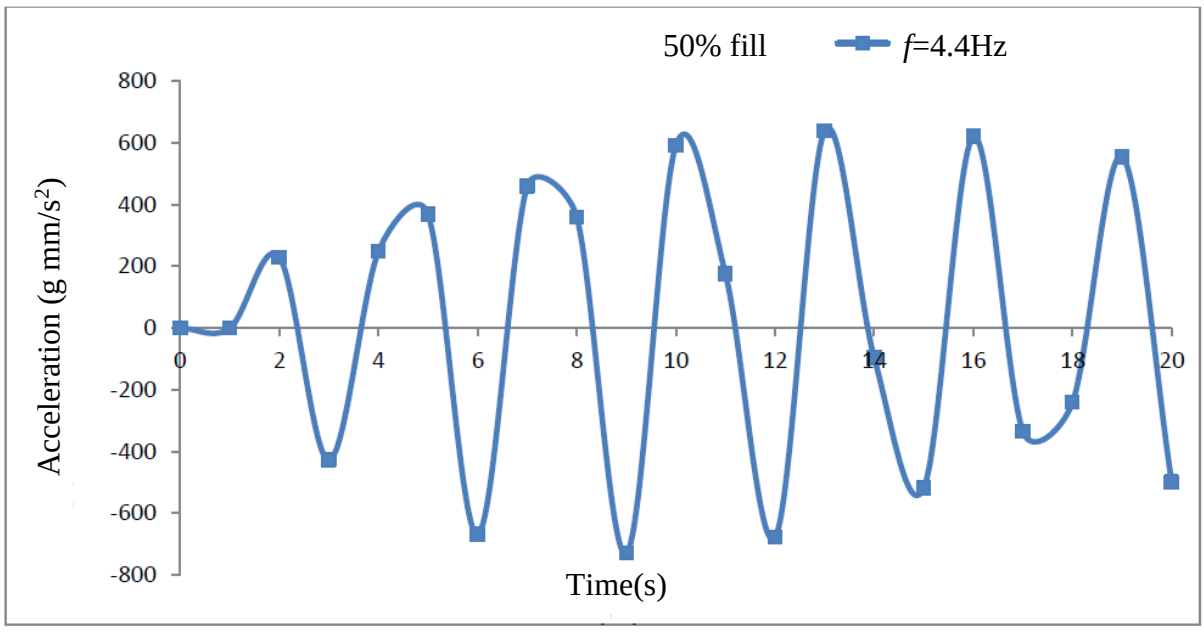

Figure 6.6: Accelerations at 50% fill at frequency 4.4Hz

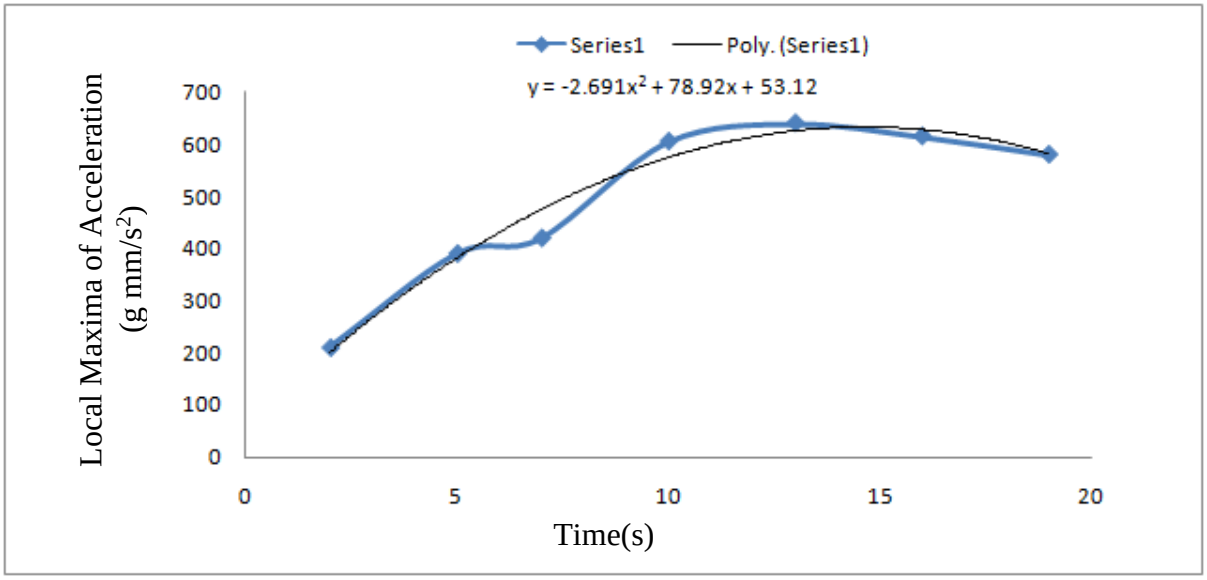

Figure 6.7: Trend line for local maxima of acceleration at 50% fill at frequency 4.4Hz

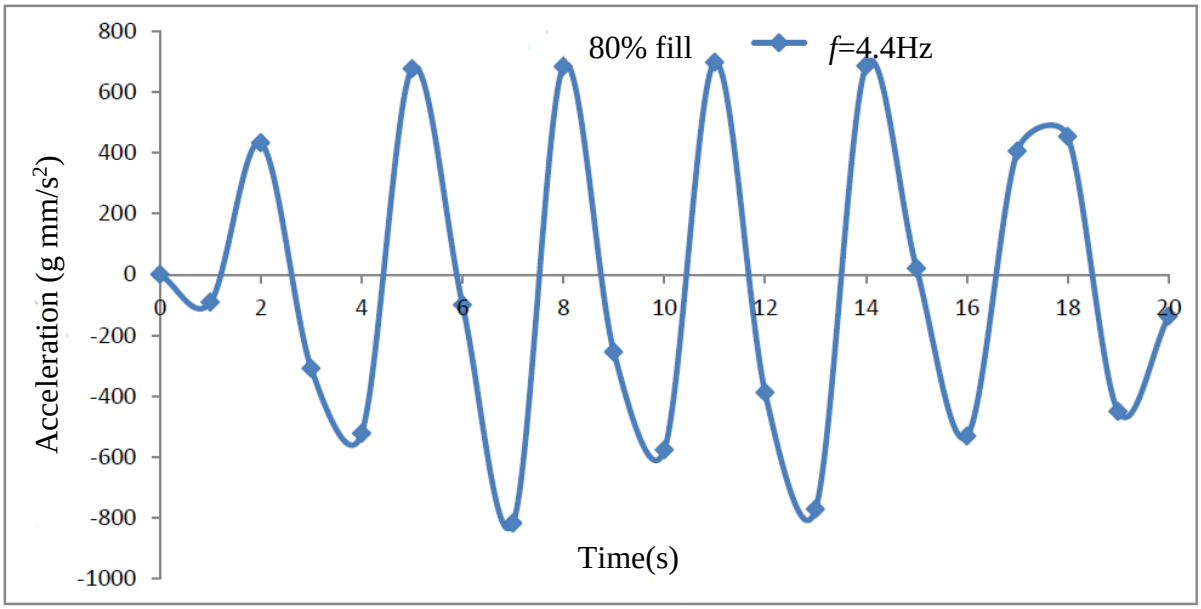

Figure 6.8: Accelerations at 80% fill at frequency 4.4Hz

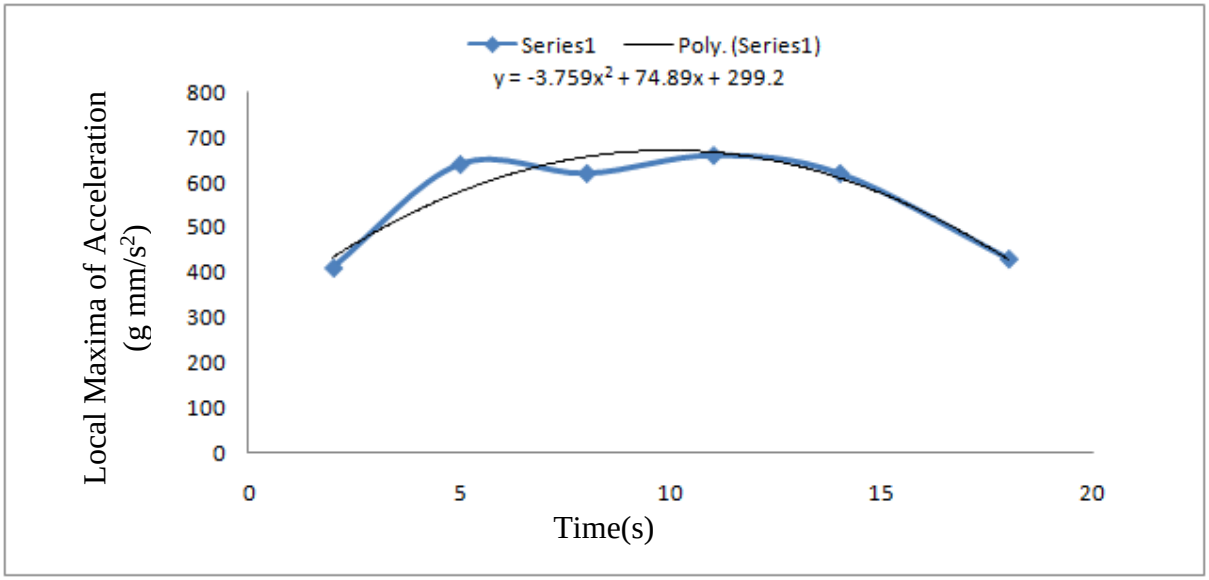

Figure 6.9: Trend line for local maxima of acceleration at 80% fill at frequency 4.4Hz

6.2.2 Fig 6.10 shows the comparison of accelerations for 50% fill and 80% fill condition, when the tank is seismically excited by frequency of 4.4Hz without baffle.

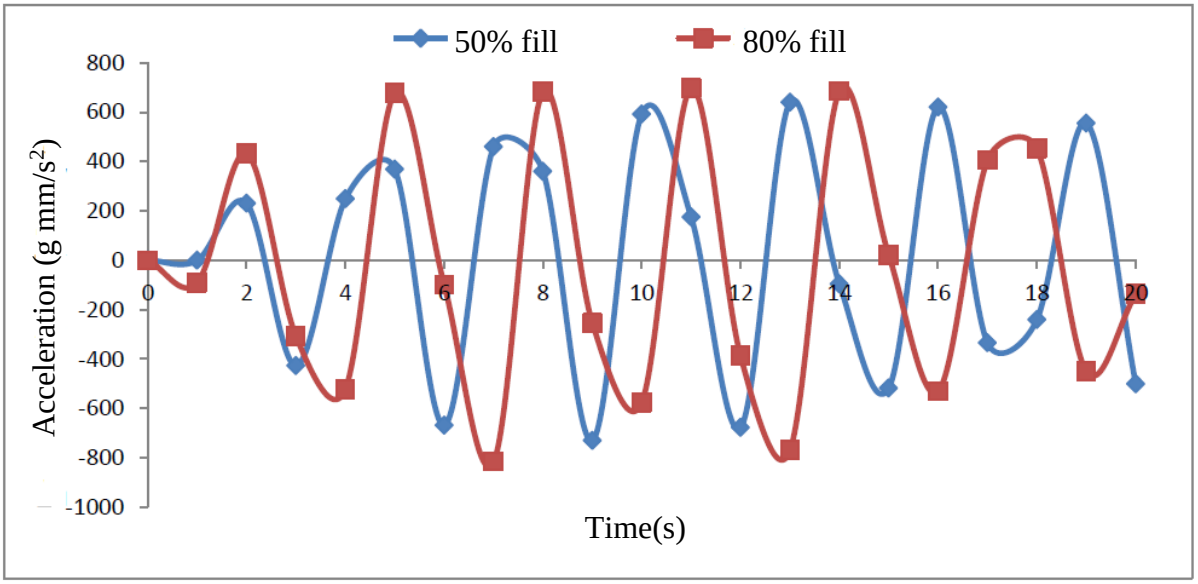

Figure 6.10: Accelerations at 50% and 80% fill at frequency 4.4Hz

From above graphs it can be observed that when the tank is excited by frequency of second mode, for accelerations the maximum amplitude is higher at high fill level, because as the frequency increases the higher fill level of fluid sloshes heavily than lower fill level.

6.2.3 Fig 6.11 shows the comparison of accelerations at frequencies of 2.8Hz and 4.4Hz at 50% fill without baffle.

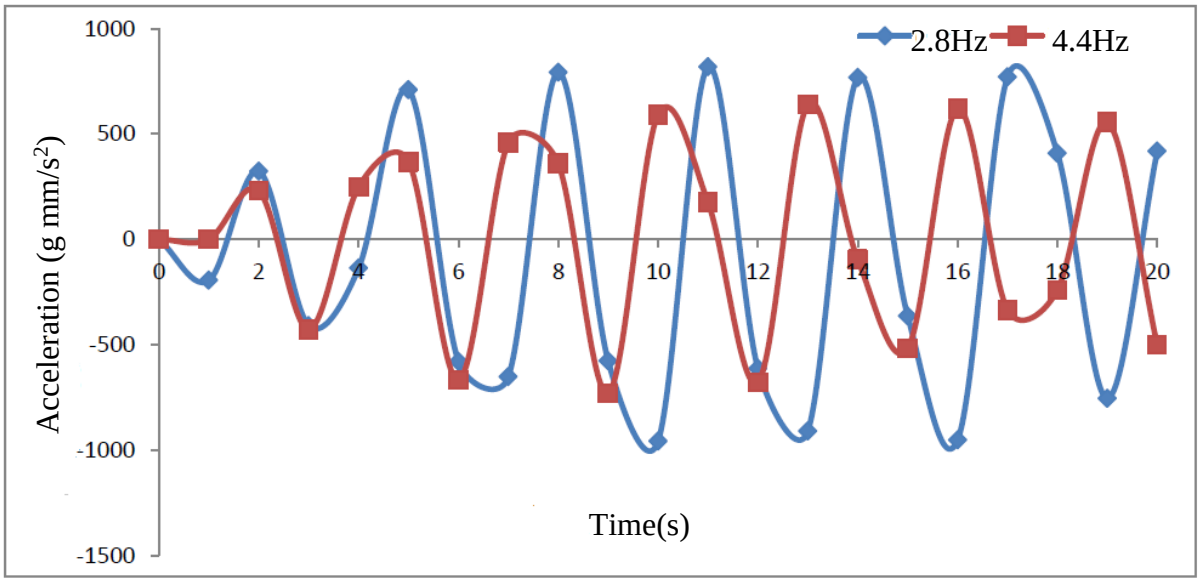

Figure 6.11: Accelerations at frequencies 2.8Hz and 4.4Hz at 50% fill

From fig 6.11, it can be observed that when the tank is seismically excited by higher frequency i.e. at second mode of the tank, the tank wall suffers lesser degree of forces and the variation of amplitudes is much less than the case of lower frequency i.e. at first mode. It happens because at first mode the height of the sloshing liquid is more.

6.3 CASE 3: When the tank is subjected to seismic excitation of frequency 2.8Hz with baffle height 0.3m

6.3.1: Fig 6.12 & 6.14 show the variations of accelerations at 50% and 80% fill when tank is equipped with baffle of height 0.3m and the tank is seismically excited by frequency of 2.8Hz. Fig 6.13 and fig 6.15 shows the graph for the local maxima of acceleration obtained from fig 6.12 and fig 6.14. It also provides the trend line and their equation for the respective cases.

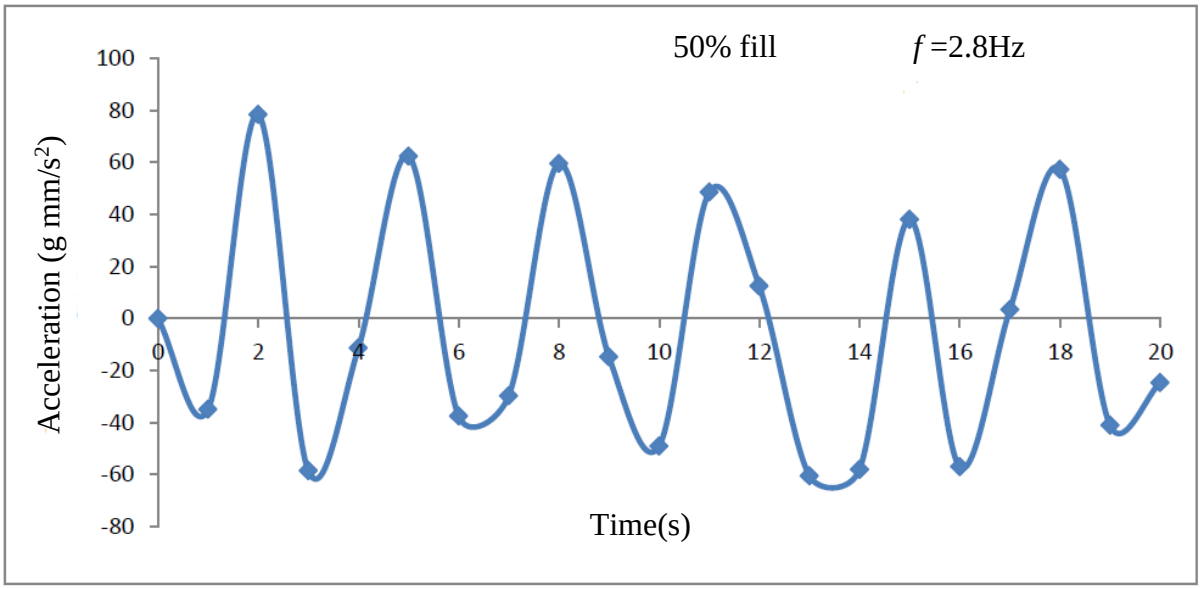

Figure 6.12: Accelerations at 50% fill at frequency 2.8Hz

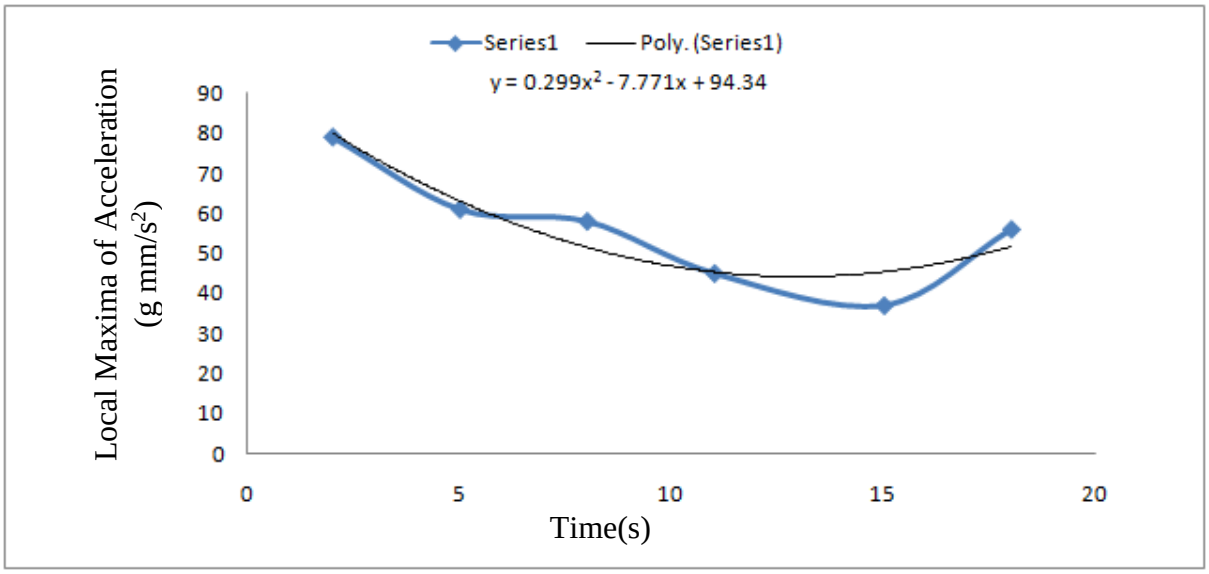

Figure 6.13: Trend line for local maxima of acceleration at 50% fill at frequency 2.8Hz

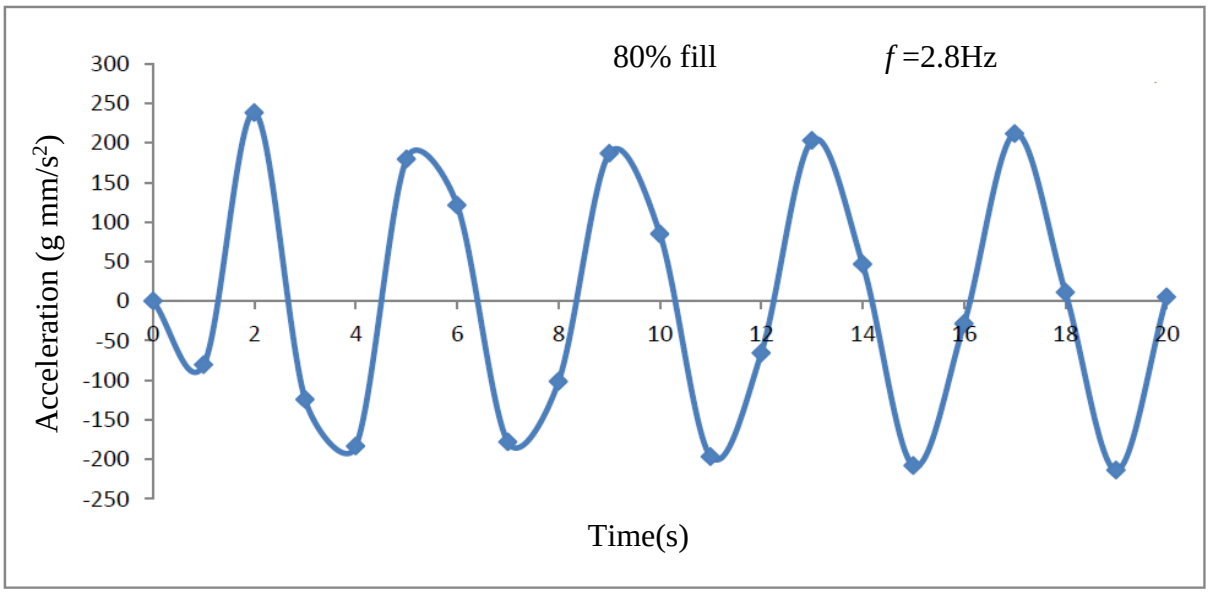

Figure 6.14: Accelerations at 80% fill at frequency 2.8Hz

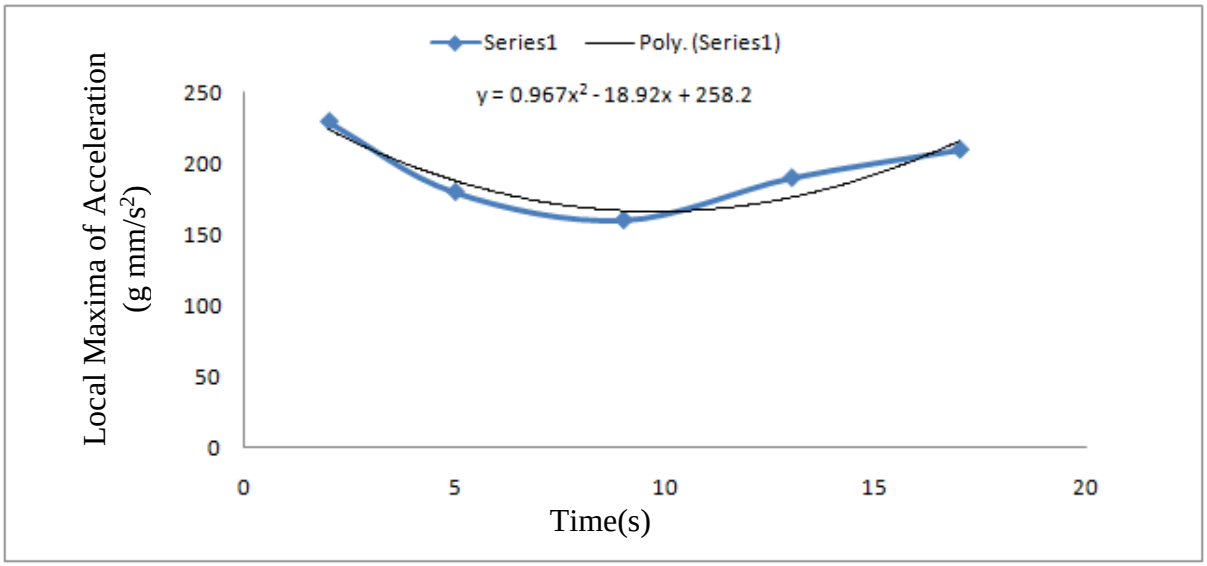

Figure 6.15: Trend line for local maxima of acceleration at 80% fill at frequency 2.8Hz

6.3.2 Fig 6.16 shows the comparison of accelerations for 50% fill and 80% fill condition, when the tank is seismically excited by frequency of 2.8Hz and is equipped with baffle of height 0.3m.

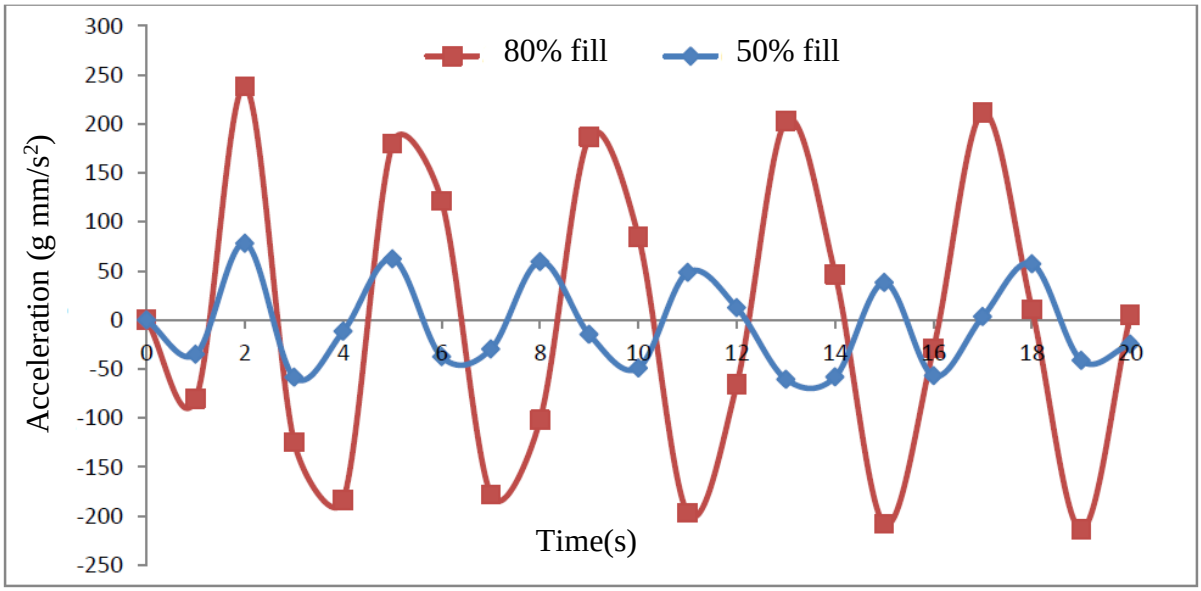

Figure 6.16: Accelerations at 50% and 80% fill at frequency 2.8Hz

Above graph in fig 6.16 shows that, when the tank is equipped with baffle of height 0.3m, tank having fill level 50% observe less acceleration i.e. force than 80% fill because for 50% maximum part of slosh movement is affected by baffle as compared to the 80% fill case.

6.4 CASE 4: When the tank is subjected to seismic excitation of frequency 4.4Hz with baffle height 0.3m

6.4.1: Fig 6.17 & 6.19 show the variations of accelerations at 50% and 80% fill, when tank is equipped with baffle of height 0.3m and the tank is seismically excited by frequency of 4.4Hz. Fig 6.18 and fig 6.20 shows the graph for the local maxima of acceleration obtained from fig 6.17 and fig 6.19. It also provides the trend line and their equation for the respective cases.

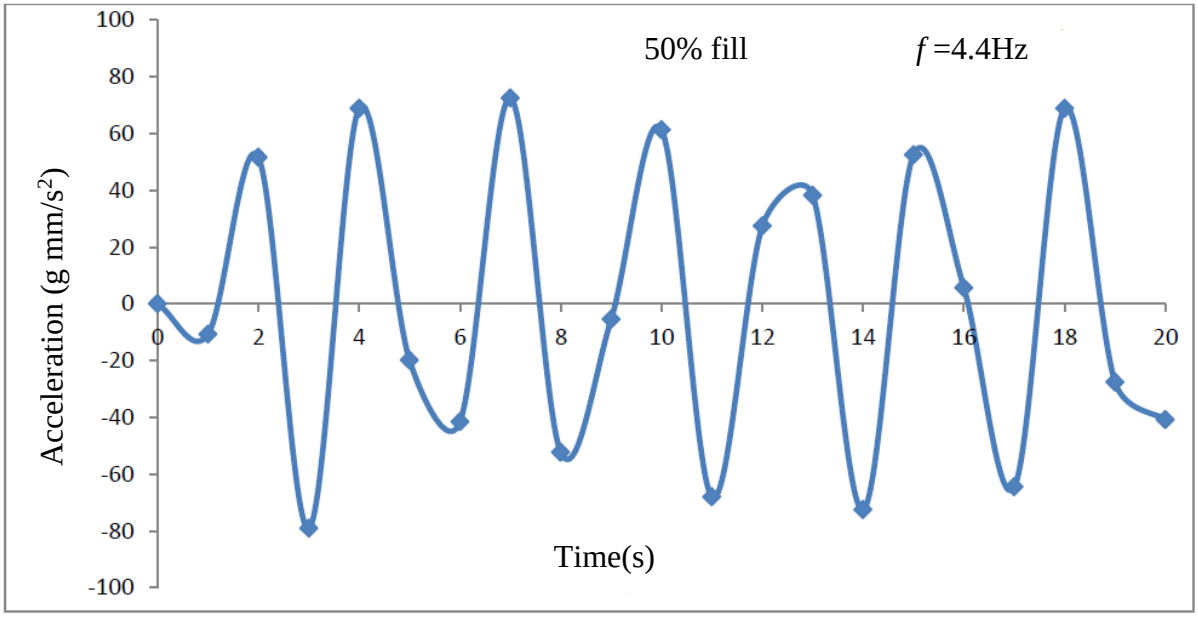

Figure 6.17: Accelerations at 50% fill at frequency 4.4Hz

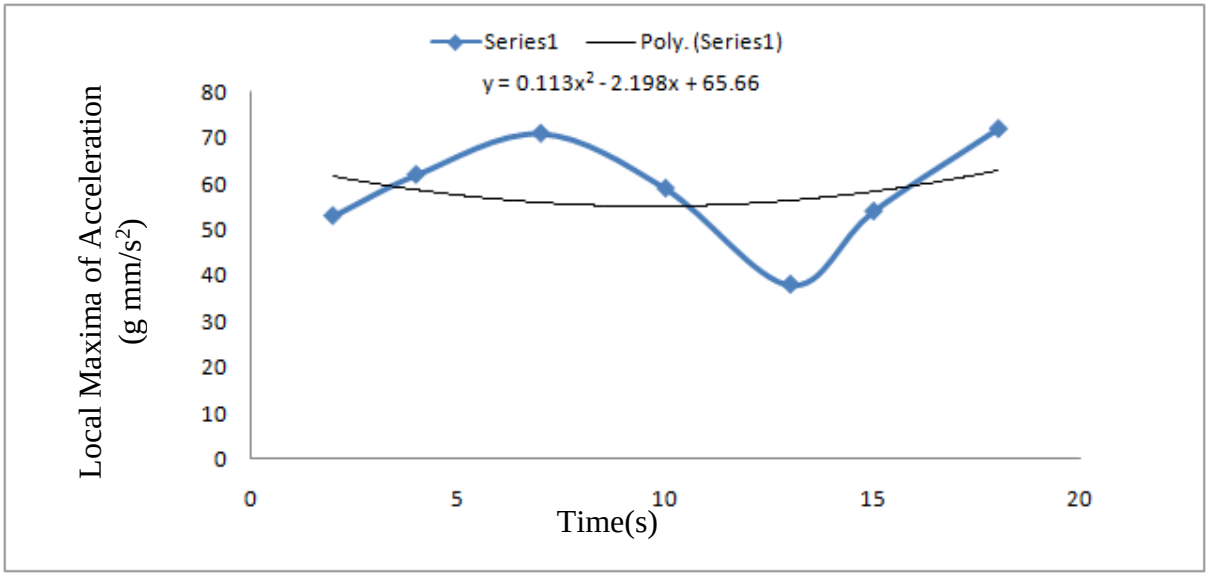

Figure 6.18: Trend line for local maxima of acceleration at 50% fill at frequency 4.4Hz

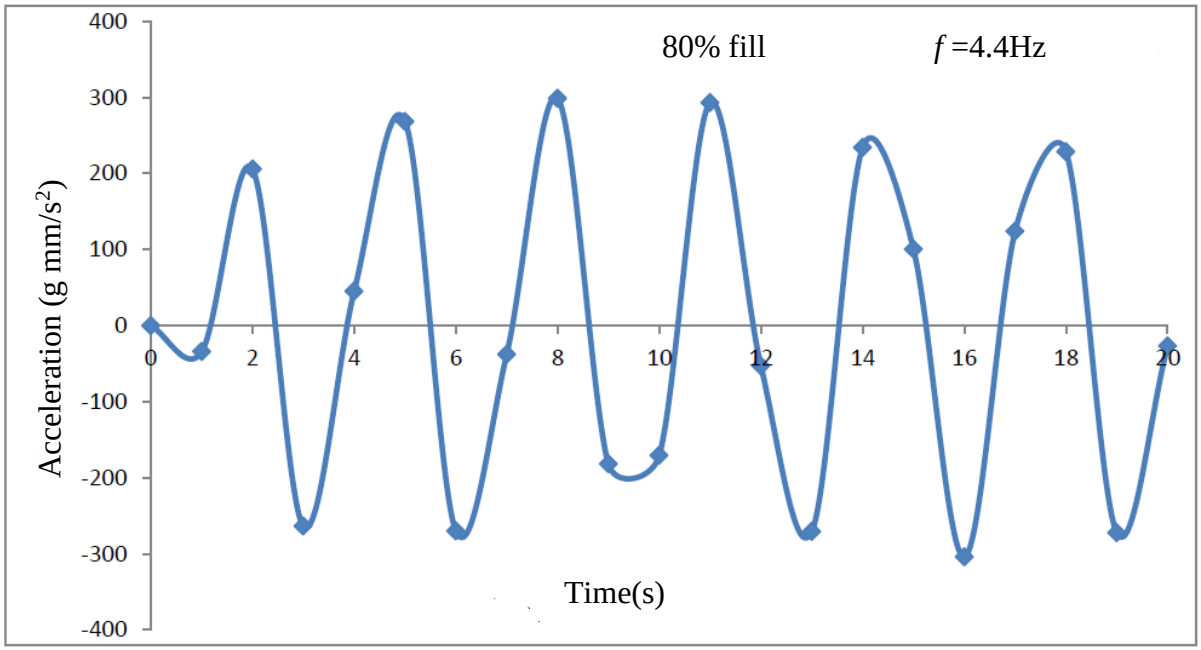

Figure 6.19: Accelerations at 80% fill at frequency 4.4Hz

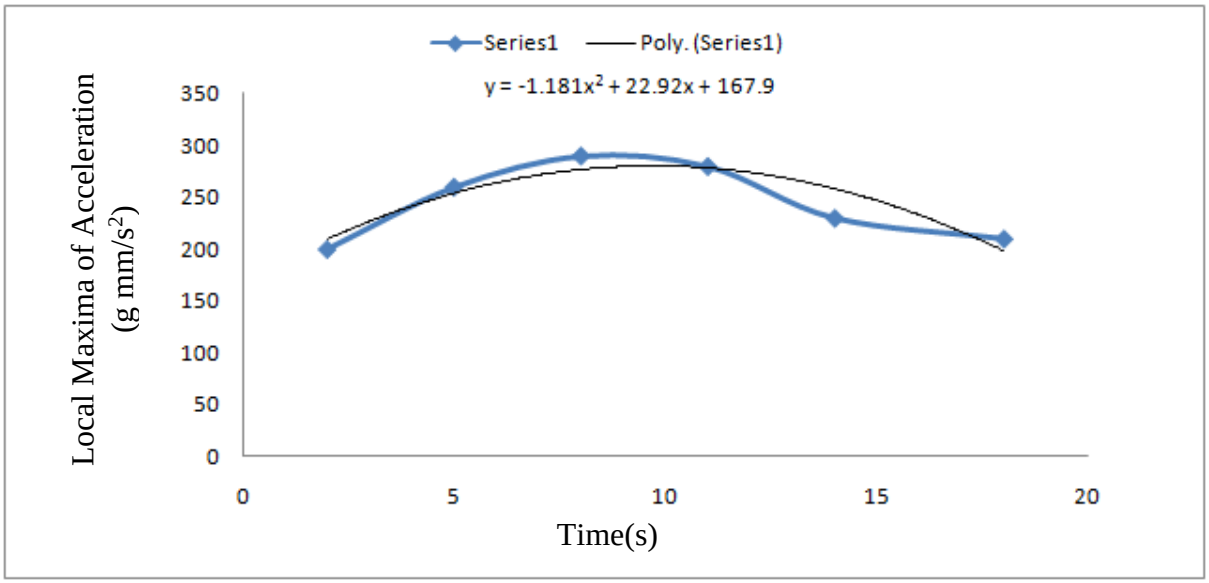

Figure 6.20: Trend line for local maxima of acceleration at 80% fill at frequency 4.4Hz

6.4.2 Fig 6.21 shows the comparison of accelerations for 50% fill and 80% fill condition, when the tank is seismically excited by frequency of 4.4Hz and is equipped with baffle of height 0.3m.

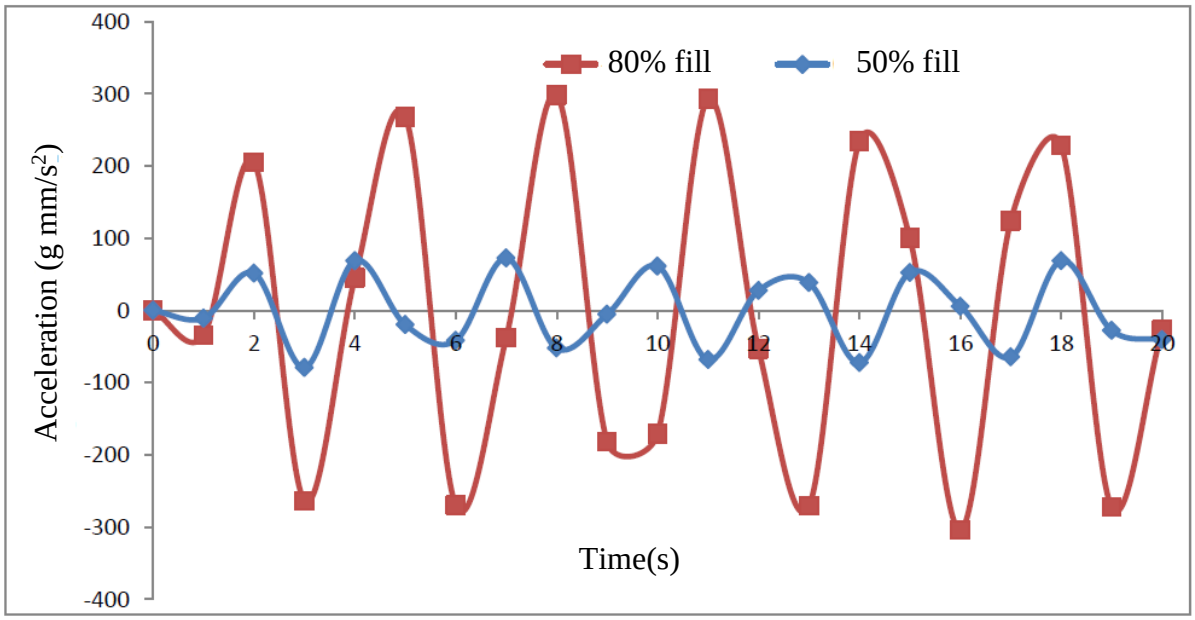

Figure 6.21: Accelerations at 50% and 80% fill at frequency 4.4Hz

Above graph in fig 6.21 shows that, when the tank is equipped with baffle of height 0.3m and is excited by higher excitation frequency that of second mode, tank shows almost similar behavior as that of frequency at first mode. Tank having fill level 50% suffer less acceleration than 80% fill because for 50% maximum part of slosh movement is affected by baffle as compared to the second case.

6.5 CASE 5: Comparison of accelerations at natural frequency 2.8Hz with and without baffle at 50% and 80% fill

6.5.1: Fig 6.22 variations of accelerations at 50% fill, when tank is equipped with baffle of height 0.3m and 0.4m & without baffle, and the tank is seismically excited by frequency of 2.8Hz.

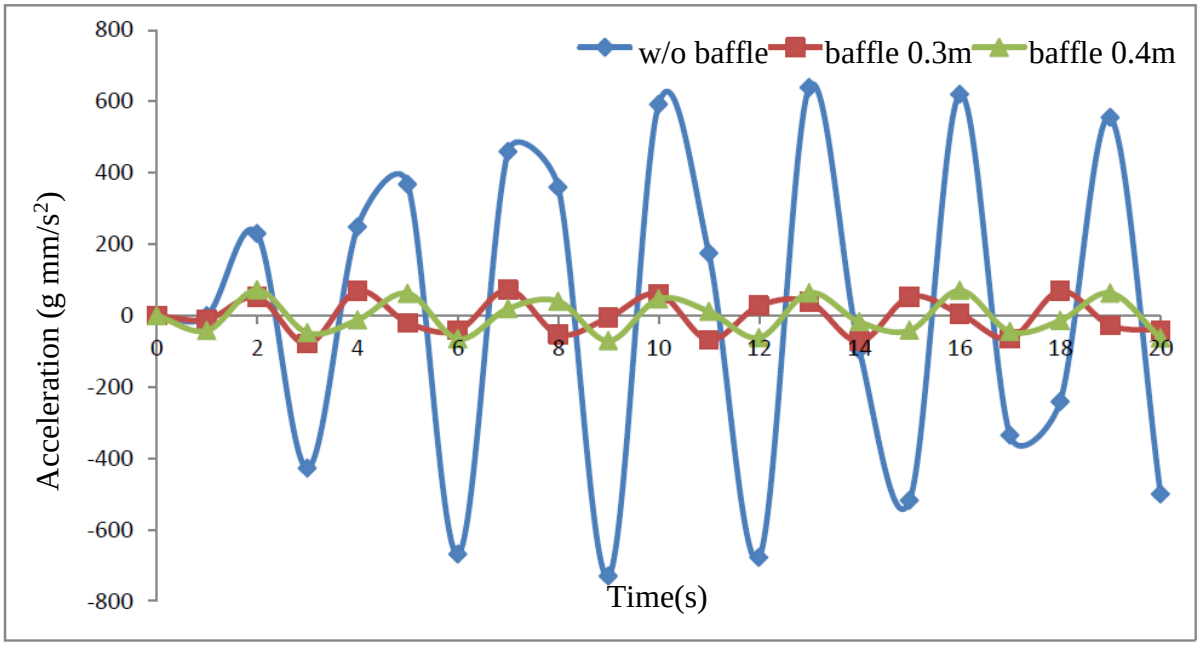

Figure 6.22: Accelerations at 50% fill at frequency 2.8Hz with and without baffle

6.5.2: Fig 6.23 variations of accelerations at 80% fill, when tank is equipped with baffle of height 0.3m and 0.4m & without baffle, and the tank is seismically excited by frequency of 2.8Hz.

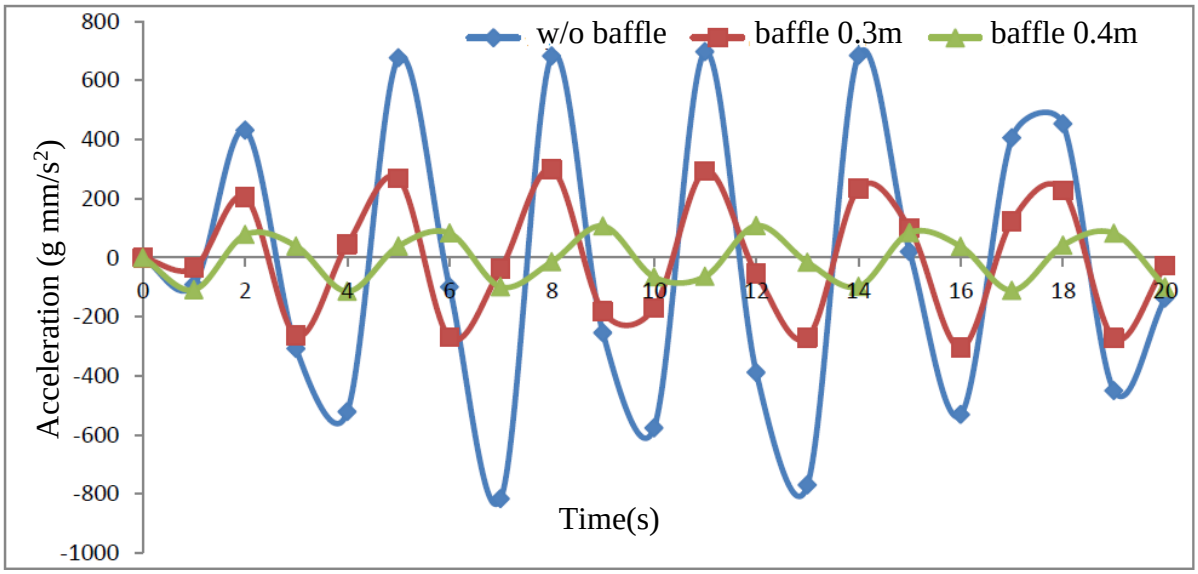

Figure 6.23: Accelerations at 80% fill at frequency 2.8Hz with and without baffle

From above two graphs, it can be observed that when tank is excited by frequency of first mode, application of baffles is largely reducing the slosh impact on wall and provide sufficient damping. When the height of baffle is equal to fill level of tank i.e. 50% fill level, sloshing behavior is considerably reduced and becomes almost linear and does not create higher impact as compared to baffle with height 0.3m or without baffle in case of 80% fill level.

6.6 CASE 6: Comparison of accelerations at natural frequency 4.4Hz with and without baffle at 50% and 80% fill

6.6.1: Fig 6.24 variations of accelerations at 50% fill, when tank is equipped with baffle of height 0.3m and 0.4m & without baffle, and the tank is seismically excited by frequency of 4.4Hz.

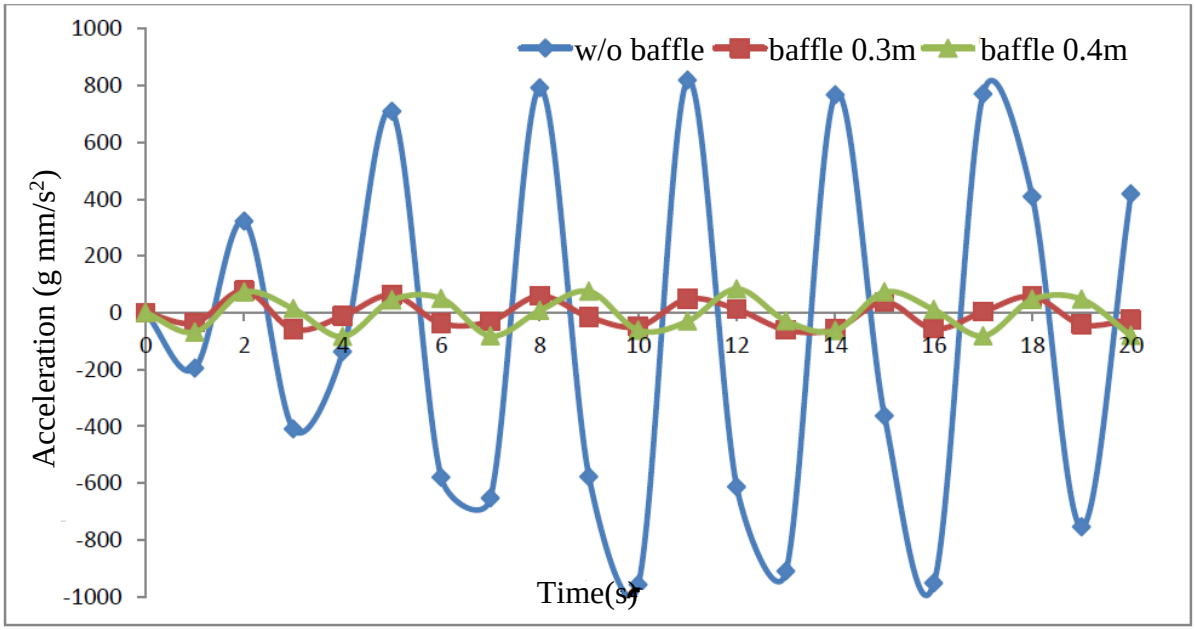

Figure 6.24: Accelerations at 50% fill at frequency 4.4Hz with and without baffle

6.6.2: Fig 6.25 variations of accelerations at 80% fill, when tank is equipped with baffle of height 0.3m and 0.4m & without baffle, and the tank is seismically excited by frequency of 4.4Hz.

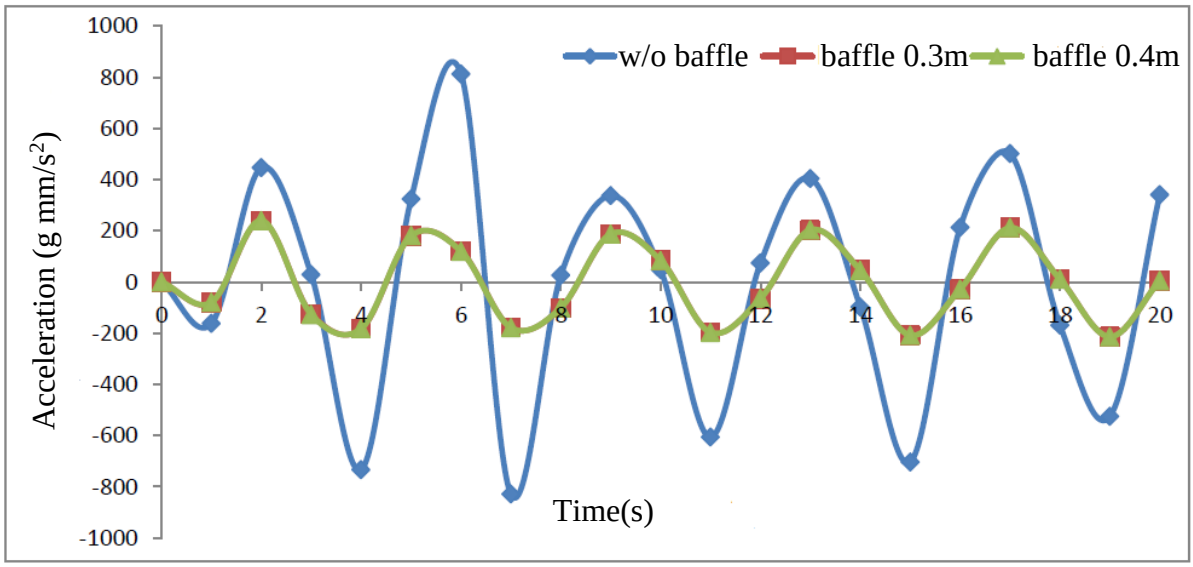

Figure 6.25: Accelerations at 80% fill at frequency 4.4Hz with and without baffle

From above two graphs, it can be observed that when tank is excited by frequency of second mode, the application of baffles are largely reducing the slosh impact on the wall and provide sufficient damping. When the height of baffle is equal to fill level of tank i.e. 50% fill level, sloshing behavior is considerably reduced and becomes almost linear and does not create higher impact as compared to baffle with height 0.3m or without baffle in case of 80% fill level. Here it can also be observed from graph in figure 6.25 that when the height of the baffle is less than that of the fill levels the effect of baffles on sloshing is less prominent. It can be seen that the variation of acceleration for the case 0.3m and 0.4m height baffles is similar when the fill level is 80% i.e. more than the baffles height.

CHAPTER 7

CONCLUSIONS

7.1 Conclusions

Following are the conclusions of this study:

1) Values of frequencies based on mathematical model [25] are found to create resonance conditions in the experimental model.
2) It is observed that the liquid inside the rectangular water tank may be excited at calculated frequencies to form standing waves.
3) Acceleration values observed with the help of accelerometers fixed at different locations at a side of the water tank are found to be different.
4) It is seen that the effect of baffle height is an important parameter to control acceleration and consequently the forces on the sides of the tank. For example in the case of accelerations at 50% fill at frequency 2.8Hz and 0.4m high baffle(figure 6.23) is seen to be most effective in reducing acceleration, followed by 0.3m high baffle.
5) It is observed that height of water in the tank is an important parameter concerning sloshing of liquid. Figure 6.22 and figure 6.23 show the acceleration values for baffled cases may be quite different for different fill levels.
6) Frequency of earthquake excitation also has been found to be an important parameter. In figure 6.25, effectiveness of both the baffles has been found to be the same regardless of difference in their heights.
7) It is found that sloshing is reduced considerably with the help of baffles. Baffles decrease the velocity of the water flow which tries to hit the wall with high velocity. This is observed by comparing the average accelerations of water in without baffle and baffled cases.
8) The time required to generate maximum velocity and acceleration is also increased with the use of baffles. This may indicate effect of duration of earthquake on sloshing of liquid.

9) The width of the baffle does not influence the sloshing [13]. The baffle has greater effect over sloshing when the fluid height is less than or equal to the baffle height. The effect of baffle on sloshing is less prominent when fluid height is more than that of baffle. This is because baffle is completely submerged in water.
10) Types of baffles in terms of its material, thickness, shape of openings, percentage of opening area seem to be important parameters.
11) Different maximum positive and negative values of acceleration are found in various acceleration v/s time graphs drawn. It may be because of various factors including stiffness of the tank wall, duration of experiment etc.

7.2 Scope of future work

Since sloshing patterns provide visual aid for the preliminary study, it will help to pursue the study further for analyzing the phenomena. This study will also lend insight into future scope of optimizing the shape of the tank and arrangement of baffle plates in the tank.

It is concluded that baffles are an effective means to reduce the intensity of sloshing effects. However, baffles can alter the characteristics of the structure model and will increase its total weight. There are many design variables while using baffles such as size, number, interval, installation position having an effect on sloshing. All these factors can be studied in future work.

REFERENCES

[1] H. Mirzabozorg, M. A. Hariri-Ardebili, R. Nateghi A, "Free Surface Sloshing Effect on Dynamic Response of Rectangular Storage Tanks", American Journal of Fluid Dynamics 2012, 2(4): 23-30 DOI: 10.5923/j.ajfd.20120204.01

[2] Chandan D. Chaudhari, Asst. Prof Prashant D.Deshmukh, Swapnil S. Kulkarni, "Assessing Sloshing Effect of Fluid in Tanker Geometry Through Deployment of Cae", Chaudhari, et al, International Journal of Advanced Engineering Research and Studies E-ISSN2249–8974

[3] Nam-Gyu Kim, Choon-Gyo Seo, Se-Hoon Kim Jong-Han Lee and Jong-Jae Lee, "Effective Hydrodynamic Analysis Methodology for Fluid Storage Tanks in Nuclear Power Plant", 2012 International Conference on Power and Energy Systems Lecture Notes in Information Technology, Vol.13

[4] Wei Wang, Yeping Xiong, "Minimising the sloshing impact in membrane LNG tank using a baffle", Proceedings of the 9th International Conference on Structural Dynamics, EURODYN 2014 Porto, Portugal, 30 June - 2 July 2014 A. Cunha, E. Caetano, P. Ribeiro, G. Müller (eds.) ISSN: 2311-9020; ISBN: 978-972-752-165-4

[5] Allan Conrad, "Hydrodynamic forces induced in fluid containers by earthquakes", California institute of technology Pasadena, California

[6] K. J. Craig · T. C. Kingsley (2007), "Design optimization of containers for sloshing and impact", DOI 10.1007/s00158-006-0038-6. Vol 33: 71–87

[7] Dr. O. R. Jaiswal, "Review of Code Provisions on Design Seismic Forces for Liquid Storage Tanks", Document No. :: IITK-GSDMA-EQ01-V1.0

[8] Sudhir K. Jain, O R Jaiswal, "IITK-GSDMA Guidelines for Seismic Design of Liquid Storage Tanks", National Information Center of Earthquake Engineering Indian Institute of Technology Kanpur

[9] S. K. Jangave, Dr. P. B. Murnal, " Structural Assessment of Circular Overhead Water Tank Based on Frame Staging Subjected to Seismic Loading", (ISSN 2250-2459, ISO 9001:2008 Certified Journal, Volume 4, Issue 6

[10] Koli G.C., A.A.Katkar, " Design & Analysis of Tanker for Reduction of Sloshing Effects", IJEIT Volume 2, Issue 2

[11] Roshan Ambade, Rajesh Kale, " CFD Analysis of Sloshing Within Tank", ISSN:2321-1156 International Journal of Innovative Research in Technology & Science(IJIRTS)

[12] IS 1893 (Part 1):2002, "Criteria for earthquake resistant design of structures", Bureau of Indian Standards, New Delhi.

[13] R. Thundil Karuppa Raj, T. Bageerathan and G. Edison, "Design of Fuel Tank Baffles to Reduce Kinetic Energy Produced by Fuel Sloshing and to Enhance The Product Life Cycle", ISSN 1819-6608 ARPN Journal of Engineering and Applied Sciences

[14] Ali Yosefi Samangany, Reza Naderi, Mohammad Hosein Talebpur2Hadi Shahabi far, "Static and Dynamic Analysis of Storage Tanks Considering Soil-Structure Interaction", International Research Journal of Applied and Basic Sciences ISSN 2251-838X / Vol, 6 (4): 515-532 Science Explorer Publications

[15] Bojja.Devadanam, M K MV Ratnam, Dr.U RangaRaju, "Effect of Staging Height on the Seismic Performance of RC Elevated Water Tank", International Journal of Innovative Research in Science, Engineering and Technology Vol. 4, Issue 1

[16] S. Hashemi, M.M.Saadatpour, M.R.Kianoush, (2013), "Dynamic behavior of flexible rectangular fluid containers", Thin Walled Structures. Vol 66: 23–38

[17] Jeff D. Tippmann, Sharat C. Prasad, and Parthiv N. Shah, "2-D Tank Sloshing Using the Coupled Eulerian-LaGrangian (CEL) Capability of Abaqus/Explicit", ATA Engineering, Inc. San Diego, CA 92130 Dassault Systèmes Simulia Corp. 166 Valley Street, Providence, RI 02909

[18] Mr. G.C. Koli, Prof.V.V.Kulkarni, "Simulation of Fluid Sloshing in a Tank", Proceedings of the World Congress on Engineering 2010 Vol II WCE 2010

[19] "Fluid structure interaction effects on and dynamic response of pressure vessels and tanks subjected to dynamic loading", Prepared by The Steel Construction Institute for the Health and Safety Executive 2007

[20] Lin P (2008). "Numerical modeling of water waves", Taylor & Francis, London.

[21] P.K.Panigrahy, U.K.Saha, D.Maity, (2009), "Experimental studies on sloshing behavior due to horizontal movement of liquids in baffled tanks", Ocean Engineering. Vol 36:213–222

[22] M. A. Goudarzi · S. R. Sabbagh-Yazdi · W. Marx, (2010), "Investigation of sloshing damping in baffled rectangular tanks subjected to the dynamic excitation", Bull Earthquake Eng. Vol 8:1055–1072

[23] Mi-An Xue, Jinhai Zheng, Pengzhi Lin, (2012), "Numerical Simulation of Sloshing Phenomena in Cubic Tank with Multiple Baffles", Journal of Applied Mathematics. Vol 2012, Article ID 245702

[24] Mahmood Hosseini, Hamidreza Vosoughifar, Pegah Farshadmanesh (2013), "Simplified Dynamic Analysis of Sloshing in Rectangular Tanks with Multiple Vertical Baffles", Journal of Water Sciences Research, ISSN: 2251-7405 eISSN: 2251-7413 Vol.5, No.1: 19-30

[25] C S Manohar and S Venkatesha, "Development of experimental setups for earthquake engineering education", National Program on Earthquake Engineering Education MHRD, Government of India